Philipp Hütter

Inkjet Printed Electrochemical Transistors and Inverters

Masterarbeit

Zur Erlangung des akademischen Grades
Diplom-Ingenieur

Masterstudium Technische Chemie

Betreuer:
Assoc.Prof. Dipl.-Ing. Dr.techn. Gregor Trimmel
Institut für Chemische Technologie von Materialien
Technische Universität Graz

Graz, Juni 2012

Deutsche Fassung:
Beschluss der Curricula-Kommission für Bachelor-, Master- und Diplomstudien vom 10.11.2008
Genehmigung des Senates am 1.12.2008

EIDESSTATTLICHE ERKLÄRUNG

Ich erkläre an Eides statt, dass ich die vorliegende Arbeit selbstständig verfasst, andere als die angegebenen Quellen/Hilfsmittel nicht benutzt, und die den benutzten Quellen wörtlich und inhaltlich entnommene Stellen als solche kenntlich gemacht habe.

Graz, am …… ……..
(Unterschrift)

Englische Fassung:

STATUTORY DECLARATION

I declare that I have authored this thesis independently, that I have not used other than the declared sources / resources, and that I have explicitly marked all material which has been quoted either literally or by content from the used sources.

…… ……..
date (signature)

Abstract

With the descovery of high conducting polyacetylene in 1977 a leap forward in the research field of organic electronics was made. In this research field conductive polymers are used as active materials opening up new possible applications due to their intrinsic properties. Their simple processability at low temperatures allows for fabrication on flexible substrates. Additionally many organic materials are processable out of solution enabling the use of standard printing techniques. With these properties they pave the way to a generation of flexible, low-cost electronic devices.

In this work entirely inkjet printed electrochemical transistors (ECTs) are fabricated using poly(ethylene dioxithiophene) poly(styrene sulfonate), called PEDOT:PSS. This conducting polymer forms, together with a polyelectrolyte, an electrochemical system. This system is responsible for the functionality of the electrochemical transistors due to a voltage-induced oxidation-reduction process leading to a reversible switching of the PEDOT:PSS between two states of different conductivity.

As a starting point electrochemical transistors are shown that are fabricated with inkjet printed PEDOT:PSS and the polyelectrolyte applied by hand. On those transistors different device geometries are varied and their influence on the transistor performance is examined. Furthermore entirely inkjet printed electrochemical transistors are fabricated. On the basis of these ECTs electrochemical inverters are fabricated that are also fully inkjet printed and represent first logic gates. To evaluate the suitability for logic circuits their dynamic switching behaviour is examined.

Zusammenfassung

Mit der Entdeckung von hoch leitfähigem Polyacetylen 1977 gelang ein großer Schritt nach vorne auf dem Forschungsgebiet der organischen Elektronik. Leitfähige Polymere werden in diesem Forschungsgebiet als aktive Materialien verwendet und eröffnen mit ihren Eigenschaften neue Nutzungsmöglichkeiten. Da sie einfach und bei niedrigen Temperaturen verarbeitbar sind, ist die Verwendung flexibler Substrate möglich. Des Weiteren können viele organische Materialien in Lösung gebracht werden und lassen sich mit Standarddruckverfahren verarbeiten. Erst diese Eigenschaften machen die zukünftige Herstellung von flexiblen und preisgünstigen elektronischen Bauteilen möglich.

In dieser Diplomarbeit wird Poly(ethylen dioxithiophen) poly(styrolsulfonat), kurz PEDOT:PSS, für die Herstellung von vollständig mittels Tintenstrahldruck hergestellten elektrochemischen Transistoren verwendet. Gemeinsam mit einem Polyelektrolyt bildet dieses leitfähige Polymer ein elektrochemisches System. Dieses System steuert die Leitfähigkeit von PEDOT:PSS durch eine spannungsinduzierte, reversible Oxidations-Reduktions-Reaktion und ist dadurch für die Funktion der elektrochemischen Transistoren verantwortlich.

Zu Beginn werden Transistoren gezeigt, die aus Tintenstrahl gedrucktem PEDOT:PSS und mit der Hand aufgetragenem Polyelektrolyt hergestellt werden. Im Anschluss daran wird die Geometrie dieser Transistoren variiert und der Einfluss auf die Transistorfunktionalität untersucht. Des Weiteren werden elektrochemische Transistoren vollständig mittels Tintenstrahldruck hergestellt. Diese Transistoren sind die Grundlage für vollständig mit Tintenstrahldruck hergestellte Inverter, welche erste Logikgatter darstellen. Um deren Eignung für Schaltkreise zu evaluieren wird das dynamische Schaltverhalten dieser Inverter untersucht.

Acknowledgement

Without the help and support of people in my surrounding writing this work would have never been possible and I like to express my sincere gratitude to all of them.

First I want to thank Joanneum Research Materials – Institute for Surface Technologies and Photonics in Weiz, Austria, and its heads DI Dr. Paul Hartmann and DI Dr. Georg Jakopic for enabling this work at their institute. Especially I want to thank DI Thomas Rothländer for his ambitious supervision of my work, his excellent support and all the discussions over several cups of coffee. Furthermore I thank Mag. Dr. Barbara Stadlober for all her help solving tricky issues and her devotedly introductions into organic electronics. Sincere appreciation is also expressed to the colleagues of the research group as well as to all other members of the institute for the warm working atmosphere and fruitful discussions.

I also gratefully acknowledge Assoc.Prof. DI Dr. Gregor Trimmel for the supervision of this work.

I want to thank my family for their superior support during the whole studying time and the writing of this work. Finally I want to thank my friends for always listening and from time to time taking my mind off work.

Contents

1 Introduction

Since the discovery that the conductivity of a polymer material (polyacetylene) can be changed from semiconducting to high conducting in 1977 [1], a lot of effort has been put into the evaluation of conducting polymers and their possible applications. One field of interest, in particular in the last decade, is the research field of organic electronics. Here conducting polymers are used as active materials in applications like organic light emitting diodes (OLEDs) [2], organic thin film transistors (OTFTs) [3], organic solar cells [4] and sensors [5]. Due to their simple processability they allow for fabrication on flexible substrates like polymer foils, paper or even biological materials. In particular, relatively low process temperatures are necessary for processing (shaping, baking or polymerisation) these organic materials. The flexibility of the substrate is a prerequisite for the next generation of mobile electronic devices and macroelectronic components not being limited in their form factors. Examples for such devices are large-area flexible displays with active-matrix addressing or conformable active large-area sensor networks [6]. Another advantage of these organic materials is that they are soluble and can be processed from solution. This enables the use of standard printing techniques like inkjet printing or screen printing. Some of the liquid source materials are also patternable by nanoimprint lithography, a method that is compatible with reel-to-reel processing. The mentioned manufacturing techniques have in common that they allow for a high throughput production and thereby low fabrication costs can be achieved. Based on that, printable conductive polymers pave the way towards a number of low-cost products that are predestinated for the market of disposable electronics.

A conductive polymer that is solution-processable at low temperatures and is compatible with a variety of flexible substrates like polymer foils and paper [7], thereby uniting the advantages described before, is the doped polymer Poly(3,4-ethylenedioxythiophene) poly(styrenesulfonate) or PEDOT:PSS. Accordingly, PEDOT:PSS is used as an active material in capacity- and transistor-based printed sensors [8], in organic transistor based circuits [9], in electrochromic displays and as interface layer in organic solar cells and light-emitting diodes [10].

A specific application of PEDOT:PSS is the use in electrochemical transistors (ECTs). Here the PEDOT:PSS plays the crucial part of the electrochemical system thus bearing the functionality of the transistors. The working principle of such electrochemical transistors is based on a voltage-induced oxidation-reduction process of PEDOT:PSS, thus resulting in a switching between two states of different conductivity. In addition, PEDOT:PSS based ECTs are potentially compatible with printing techniques and thereby allow for high throughput fabrication. With the possibility of being fabricated and operated on flexible substrates at low costs the main advantages of organic electronics are realized with electrochemical transistors.

1.1 Project scope of this work

The goal of this work is the fabrication of fully inkjet printed electrochemical transistors (ECTs). Furthermore these transistors will constitute the basic elements of electrochemical inverters.

To reach that goal the suitability of inkjet printed PEDOT:PSS for the fabrication of ECTs is evaluated first (Chapter 4.1.1). With this confirmed, different transistor geometries are varied and the influence on the transistor performance is examined (Chapter 4.1.3). Then the possibility to process the electrolyte per inkjet printing is verified (Chapter 4.2). As a next step entirely inkjet printed ECTs are fabricated (Chapter 4.2). Based on these transistors first logic gates, made up of entirely inkjet printed inverters, are produced (Chapter 4.3). These inverters are electrically and dynamically characterized in order to determine their performance and their switching behaviour.

2 Theory

2.1 Poly(3,4-ethylene dioxythiophene) poly(styrene sulfonate)

For the fabrication of the electrochemical transistors presented in this work poly(3,4-ethylene dioxythiophene) poly(styrene sulfonate), also called PEDOT:PSS, is used as the active material. As a highly doped polymer semiconductor it is widely used as a conductive polymer that, due to its redox property, meets the requirements for building electrochemical transistors very well. The following chapter gives a brief description of the pathway from a monomer to the doped polymer. Furthermore the origin of the conductivity of PEDOT:PSS is described.

2.1.1 Syntheses of PEDOT:PSS

PEDOT:PSS is a conductive polymer, thus involving a polymerisation step during fabrication. The starting point of every polymerisation is a monomer. In the case of the synthesis of poly(ethylene dioxythiophene) (PEDOT) the monomer used as educt is ethylene dioxythiophene (EDOT). It can be synthesized in several different ways [11]. A synthesis often used in commercial applications was developed by Jonas et al. [12]. Based on this monomer a large variety of different polymerisation methods exists. Neutral undoped PEDOT is achieved for instance by dehalogenation using nickel complexes [13] or “self-oxidation” [14], although halogenated EDOT monomers are needed to enable this syntheses. A possible way to synthesize neutral undoped PEDOT from unmodified EDOT is an oxidative polymerisation with iron(III) chloride although only moderate yields are achievable [15]. Oxidated PEDOT that is already doped when the polymerisation is completed is obtained by electrochemical polymerisation [16] or by oxidative polymerisation. A prominent example for an oxidative polymerisation is the so-called BAYTRON P syntheses [17]. This polymerisation is often applied to produce PEDOT:PSS on an industrial scale because (i) the doped PEDOT:PSS is already obtained in the course of the polymerization of EDOT and (ii) water is used as the solvent. This is a big advantage

compared to fabrication processes where a polymerisation and a following doping process is necessary. Therefore a closer look at this synthesis is taken.

The BAYTRON P polymerisation is carried out at room temperature in an aqueous PSS polyelectrolyte solution using $Na_2S_2O_8$ as the oxidizing agent. The reaction scheme is shown in figure 2.1.

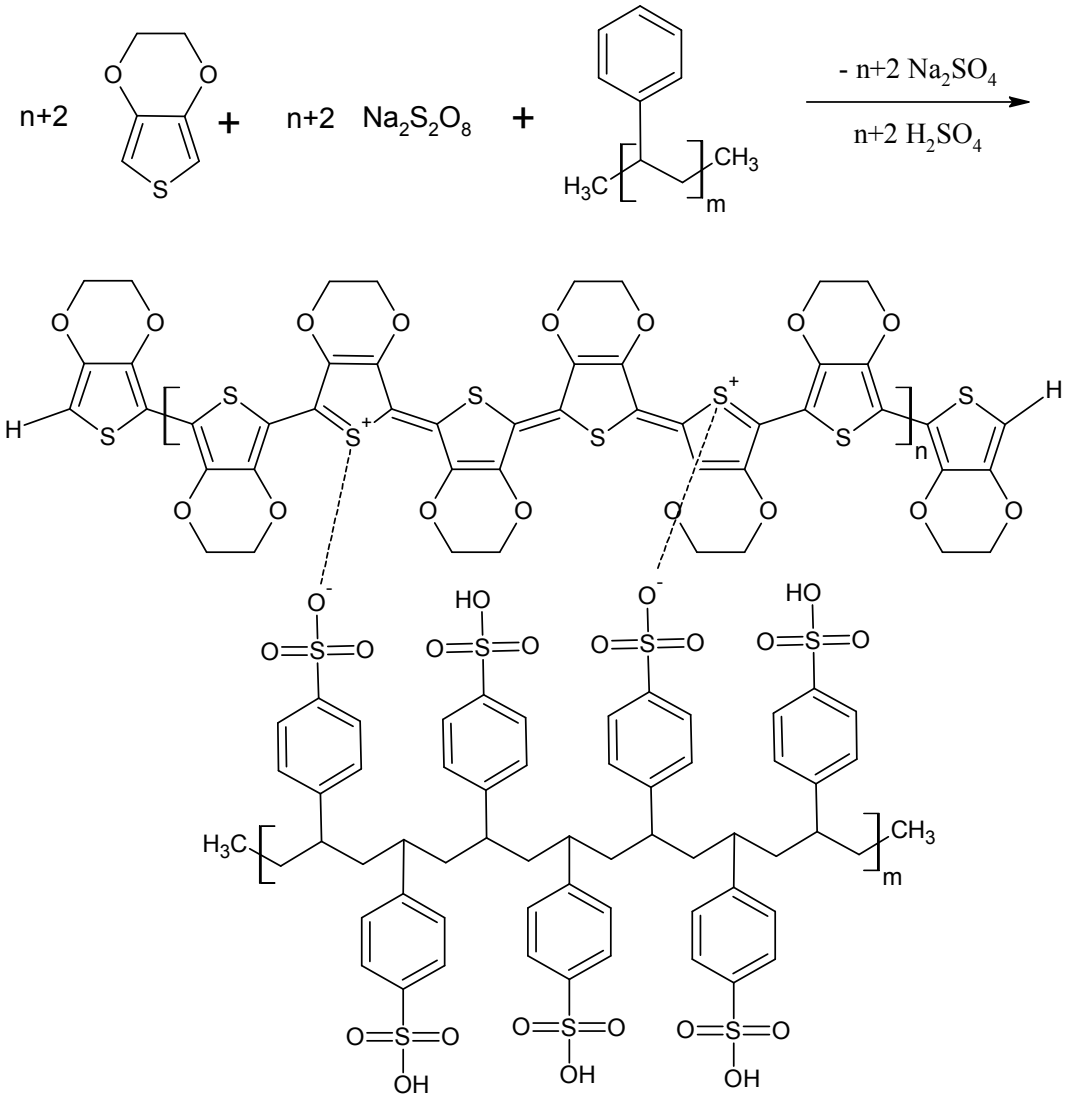

Figure 2.1: oxidative polymerisation of PEDOT [11]

The product is an aqueous PEDOT:PSS solution that can be directly processed and, when dried, forms a highly conducting, transparent, mechanically durable and in many solvents insoluble PEDOT:PSS film [18].

2.1.2 Conductivity of PEDOT:PSS [27, 37]

PEDOT is a polymer that belongs to the class of the polythiophenes and is electrically conductive due to its π-conjugated system [19]. The polymer backbone consists of carbon atoms connected by alternating single and double bonds. When two carbon atoms are forming a double bond they are sp^2 hybridized. Between the atoms an σ bond, where the electrons are strongly localized between the bonding carbon atoms, and a π bond with delocalized electrons are formed (figure 2.2).

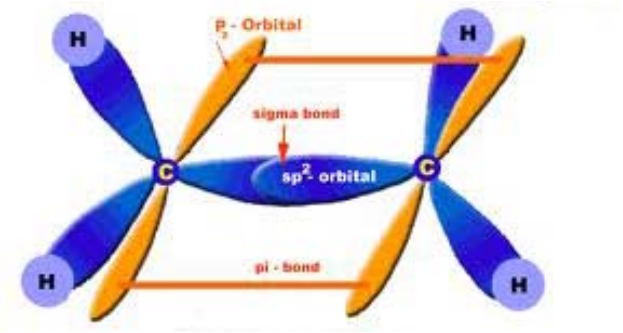

Figure 2.2: orbitals when two carbon atoms form a double bond [20]

The π bond is formed by the overlap of the $2p_z$ orbitals of the two adjacent, bonding carbon atoms. In this way a bonding π orbital and an antibonding π* orbital are formed. The electrons in these orbitals are not bound to one carbon atom, they are delocalized. When four atoms are binding, the π and π* orbitals are split up in four orbitals. This effect is repeated when two additional carbon atoms are added to the binding. In polymers, where a very large number of N carbons is added up to a polymer chain, the energy niveaus are splitted up so often that they can be considered as π and π* energy bands (see figure 2.3). Due to the structure of the conjugated polymer chain with the overlapping $2p_z$ orbitals and the alternating single and double bonds, a fully filled π band, the valence band, and an empty π* band, the conductive band, with a specific band gap are formed. For substituted polythiophenes this band gap is in the range of 2 and 4 eV [21] as is typical for π-conjugated organic semiconductors.

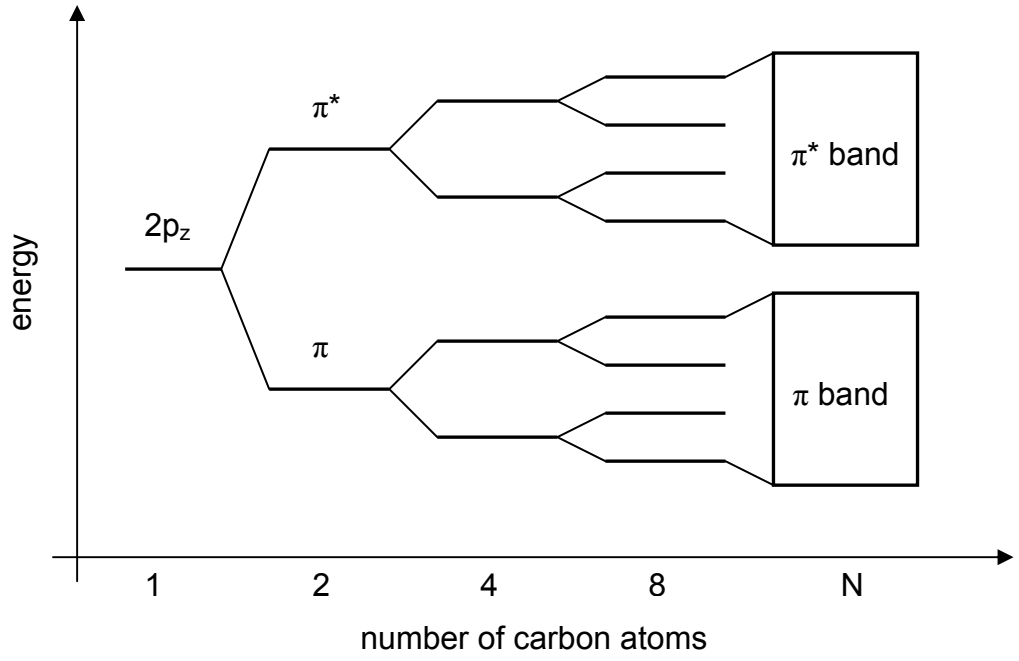

Figure 2.3: π and π* orbitals for an increasing number of bonding carbon atoms

Because the backbone of the conjugated polymer consists of alternating single and double bonds, two possibilities of arranging these bonds are given. PEDOT is a conjugated polymer with a non-degenerate ground state. Such polymers have a prefered order of bond configuration. The two possibilities in PEDOT are the aromatic and the quinoid bond configuration shown in figure 2.4 a) and b). Since the energy level of the quinoid form is higher, the aromatic form is the preferred bond configuration [22].

Figure 2.4: a) aromatic and b) quinoid form of PEDOT

When a conjugated polymer (figure 2.5 a)) is oxidized, an electron from the π-electron system is removed thus resulting in a positive charge formed on the backbone of the polymer. The charge is delocalized over a defined section of the polymer chain leading to a rearrangement of its bonding configuration. Despite of the

higher energy of the quinoid configuration, the preferred aromatic configuration is partly transferred into the quinoid configuration when the polymer is oxidized. At the carbon atoms hosting this transition, the positive charge and a corresponding free radical are localized (see arrows in figure 2.5 b)). The quinoid system is located between the positive charge and the free radical and is stabilized by them, enabling the endurance of this higher energy configuration. The combination of a positive charge, a free radical and the quinoid configuration is referred to as a polaron and is depicted in figure 2.5 b). When the conjugated polymer is further oxidized, a second polaron can be formed somewhere along the polymer chain. These two polarons can combine to a bipolaron. Such a bipolaron can also be obtained when an already existing polaron is further oxidized. As shown in figure 2.5 c) in a bipolaron the free radical is replaced by a second positive charge.

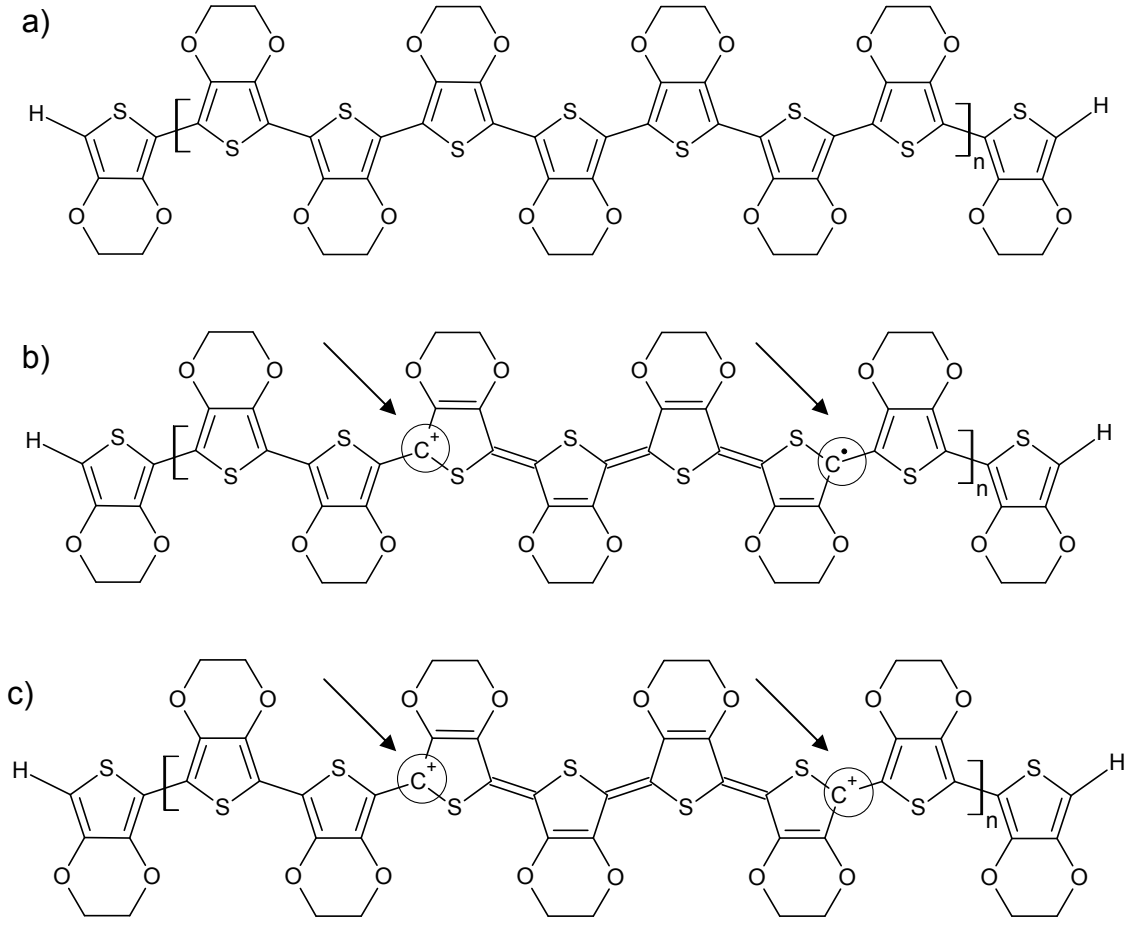

Figure 2.5: a) neutral PEDOT b) oxidized PEDOT containing a polaron c) further oxidized PEDOT containing a bipolaron

To obtain electric conductivity, the charge carriers need to move through the polymer. The mechanism of charge transport in PEDOT:PSS is still poorly understood [11]. Because a charge is able to move through the polymer when two polarons are combining to a bipolaron, it can be suggested that the charge carriers are transported along one polymer chain as a package altering the single and double bond positions as shown in figure 2.6. However, since the polymer chains have a finite length and polymer materials are not homogenious, a transfer through the whole material would not be possible in this way. Additional, the charge carriers must be transferred from one polymer chain to another to obtain an electronic conductivity throughout the whole material. This type of charge transport has been examined by the temperature dependence of the conductivity of PEDOT:PSS and described within the framework of variable range hopping [23]. In variable range hopping the charge carriers are transported through tunneling between localized states of the conjugated polymers. Accordingly charge carriers can be transported between different polymer chains thus enabling an electronic charge transport through the whole polymer.

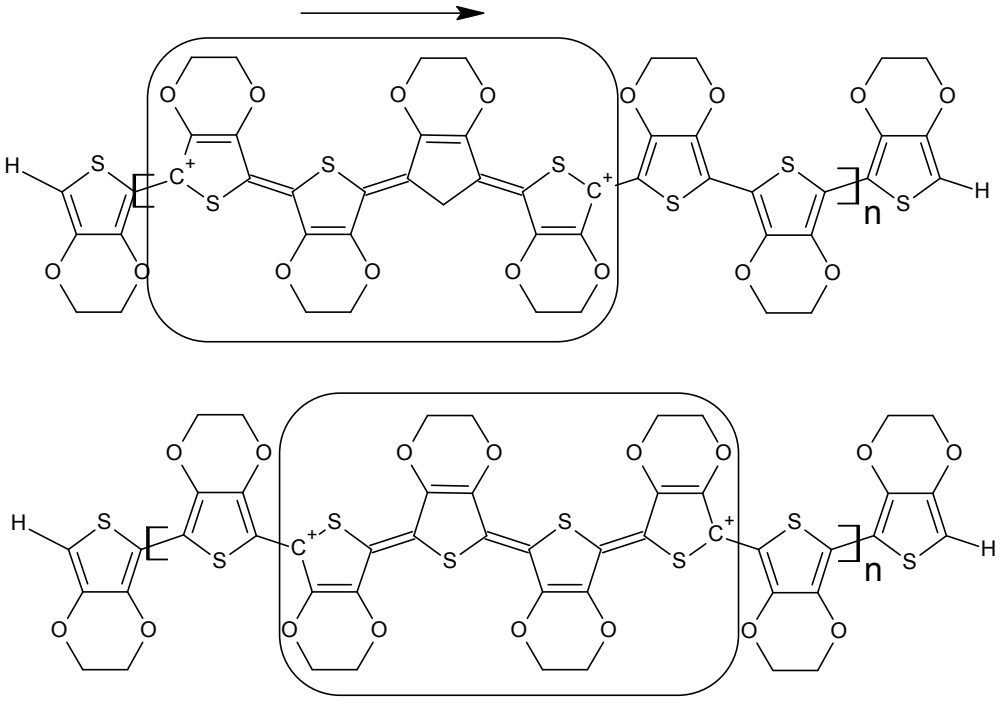

Figure 2.6: charge carriers moving along a PEDOT chain [37]

In addition to the electronic conductivity described before, polymers can show ionic conductivity. The ions can only move within a polymer if there is enough space, so-called free volume, which can be occupied by them. For large ions like PSS^- it is

difficult to find enough space, hence the transport of PSS^- in conjugated polymers is very unlikely. There is a strong influence of the ion size on its mobility in polymer materials [24].

In their pristine state most conjugated polymers act as semiconductors or insulaters due to the small number of charge carriers formed by thermal excitation. To increase the number of charge carriers and thus increase the conductivity of conjugated polymers, doping is a useful way. For example the conductivity of formerly doped PEDOT decreases in the order of 4-5 magnitudes when it gets de-doped [25]. Doping can be realized in an electrochemical or in a chemical way.
When electrochemical doping is performed electrons are transferred to and from the π system by application of an electric field. In this way the polymer backbone gets positively or negatively charged. This charge has to be balanced by a counter ion. In the case of electrochemical doping these ions are provided by a corresponding ion source, for example an electrolyte solution. Charge balancing is obtained by migration of those ions in or out of the conjugated polymer. In this way the counter ion for the doped polymer can be chosen. A scheme of the setup for electrochemical doping is shown in figure 2.7. The doping process is described by equation 2.1.

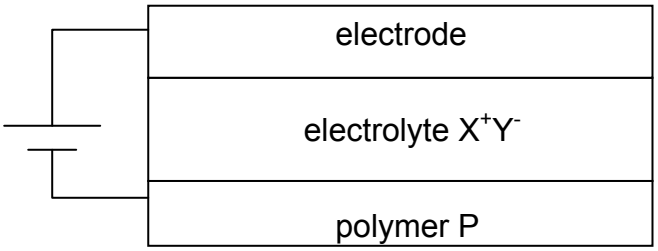

Figure 2.7: scheme of the setup for electrochemical doping

$$P^0 + X^+Y^- \leftrightarrow P^+Y^- + X^+ + e^- \qquad (2.1)$$

The behaviour of PEDOT during electrochemical doping and de-doping is described by Zykwinska et al. [26].
Chemical doping is performed by a redox reaction, leading to an electron transfer between the polymer and the dopand. During oxidation an electron is removed from the π system. An electron is added to the π system when reduction occurs. Due to that change of the number of electrons the polymer backbone gets positively or negativley charged. Similar to electrochemical doping a counter ion is needed to

balance this charge. An example for oxidative chemical doping is the reaction scheme in figure 2.1, where the doping occurs in the course of a polymerisation. With PSS^- used as the counter ion to balance the charge of the doped $PEDOT^+$, PEDOT:PSS, the conducting polymer that is used for the transistors in this work, is obtained (see figure 2.8).

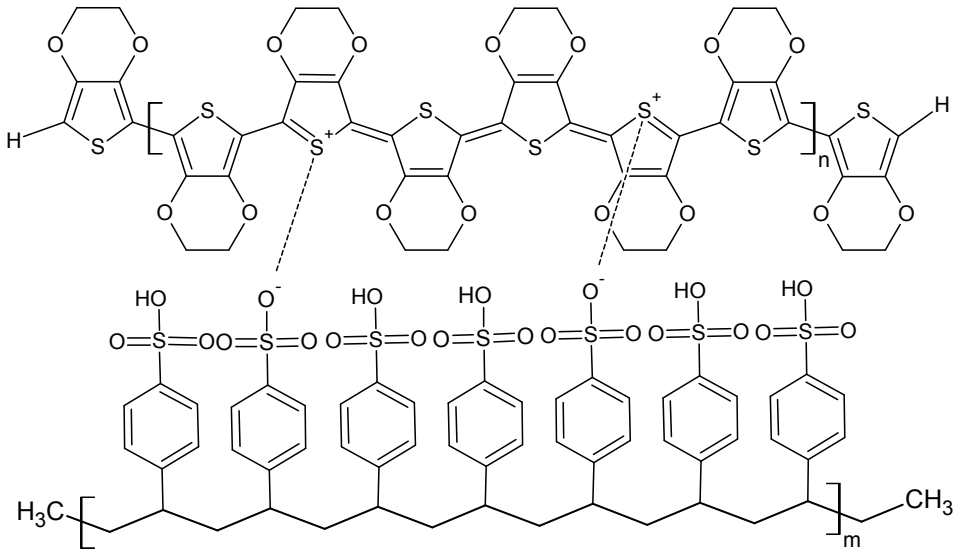

Figure 2.8: structure of PEDOT:PSS [11]

2.2 Electrolytes [27]

A generall definition for an electrolyte is that it is a chemical compound containing dissociated ions that are able to move in a specific direction when an electric field is applied [28]. These dissociated ions are responsible for the conductivity being an intrinsic property of electrolytes. Usually electrolytes are liquid, but also gelled or solid forms are possible. One way to classify them is the strength of the electrolyte, depending on the degree of dissociation. In strong electrolytes most of the ions are dissociated, leading to many free charge carriers. In weak ones most of the ions exist in the form of not dissociated ion pairs and thus are not available as charge carriers. In this way the conductivity of an electrolyte can be assessed.
Following a variety of electrolytes being relevant for the use in organic electronics is listed.

2.2.1 Electrolyte solutions

Electrolyte solutions are fabricated by dissolving a salt, consisting of an ion pair, in a liquid medium, the solvent. In the course of dissolving the salt the ion pair is split up and every ion is surrounded by solvent molecules forming a solvation shell. As a result the ions are separated and able to move in the solvent. Water is a common solvent and an electrolyte itself, although a weak one. In water a small amount of the H_2O molecules is dissociated into hydrogen ions (H^+) and hydroxide ions (OH^-). The hydrogen ions get hydrated to hydronium ions (H_3O^+) in aqueous solutions. Together with the OH^- ions the H_3O^+ ions are representing the mobile ions in water. An example where water is used in organic electronics constitutes the organic thin film transistor where water is used as the gate dielectric shown by L. Kergout et al. [29].
Because only a polar solvent and a dissolvable salt are necessary to form a electrolyte solution, a lot of possible solutions for many different applications are conceivable. One example is the electrochemical transistor presented by L. Basirico et al. where a saline solution is used as the electrolyte necessary to switch the transistor [30].

2.2.2 Polyelectrolytes

In polyelectrolytes a polar solvent like water is also needed. But instead of a salt a polymer with an electrolyte group in its polymer chain is brought into contact with the polar solvent. In the course of this solvent contact the electrolyte group can

dissociate forming the polymer electrolyte consisting of a charged polymer and a counterion. A negatively charged polymer is called polyanion and a positively charged polymer is called polycation. When a thin film of polyelectrolyte is fabricated or its solvent content is reduced, the large polyanions or –cations are immobile due to their size and only the counterions remain mobile. Like this electrolytes with only one type of moveable charged ions can be fabricated. An example for the use of a polyelectrolyte in organic electronics is the electrochemical transistors fabricated by D. Nilsson [31]. Here poly(styrene sulfonate) (PSS^-) forms the polyanion and sodium cations (Na^+) are the mobile counterions (see figure 2.9).

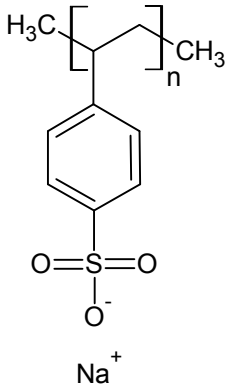

Figure 2.9: polyanion PSS^- with Na^+ as counterion

2.2.3 Polymer electrolytes

In polymer electrolytes the used solvent is a polymer. A salt is dissolved in the polymer matrix forming the moveable ions. A very common polymer electrolyte is poly(ethylene oxide) (compare figure 2.10) with dissolved sodium or lithium salt. There the cation, Na^+ or Li^+, is coordinated to the oxygen of the poly(ethylene oxide) seperating it from the anion of the salt. An example for poly(ethylene oxide) with dissolved lithium salt in use for organic electronics is the polymer electrolyte gated organic thin film transistor shown by M. J. Panzer et al. [32].

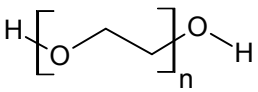

Figure 2.10: poly(ethylene oxide)

2.2.4 Ionic liquids

An ionic liquid is a salt in its liquid state. Any salt that is not decomposing or vaporizing when it is melting is usually forming an ionic liquid after its melting point. In

contrast to water that is mainly consisting of neutral molecules an ionic liquid consists of ions and transient ion pairs. An example is NaCl that is forming an ionic liquid consisting of Na^+ and Cl^- ions at its melting point of 801°C. Anions and cations of ionic liquids with a melting point below 100°C are often large, have a delocalized charge and are organic. An example for an ionic liquid is the hexafluorophosphate salt of 1-butyl-3-methylimidazolium shown in figure 2.11. In organic electronics ionic liquids are used in batteries, fuel cells and supercapacitors [33].

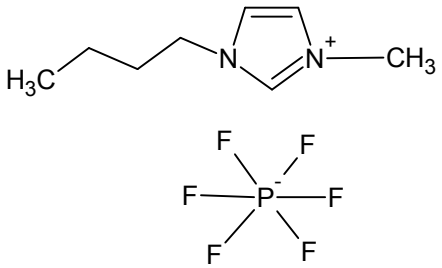

Figure 2.11: hexafluorophosphate salt of 1-butyl-3-methylimidazolium

2.2.5 Ion gels

Ion gels are ionic liquids with their ions immobilized in a polymer network. In this way the ionic liquid is macroscopically immobilized and thus easier to handle. The polymer matrix can be a block copolymer or a polyelectrolyte that is, together with the ionic liquid, resulting in an ion filled polymer matrix, the ion gel. An application for ion gels in organic electronics is the ion gel gated polymer thin film transistor using a ionic liquid immobilized in a triblock copolymer for the gate dielectric shown by J. Lee et al. [34].

2.2.6 Ionic charge transport

The charge transport mechanism in electrolytes strongly depends on the type of electrolyte. In general two reasons for moving ions in electrolytes are possible. First a gradient in concentration leading to a charge transport by diffusion and second an applied electric field leading to electro migration.

In polymer electrolytes the ion motion is coupled with the segmental motion of the polymer chain. When the mobility of the polymer chain is low due to long chains or highly ordered regions in the polymer, the mobility of the ions will be low thus leading to a low ionic conductivity. In solvents the mobility of ions is limited by the viscosity of the solvent and the size of the moving ion. These two parameters can be

summerized to a friction force that is limiting the ionic mobility and thus the ionic conductivity.

2.2.7 Electrolytes used in this work

In this work two different electrolytes are used. They will be referred to as Electrolyte 1 and Electrolyte 2. Electrolyte 1 is a polyelectrolyte using water as the solvent and PSS^- as the polyanions. The mobile counterions are dissolved Na^+ ions. This electrolyte is used due to its well known properties and the proven possibilty to fabricate electrochemical transistors utilizing this electrolyte. Additionally the low viscosity and thus the processibility by inkjet printing is a reason to use this particular electrolyte.

Electrolyte 2 is a polymer electrolyte. Due to its confidential status, the composition cannot be disclosed in this work. This electrolyte is used due to its high viscosity allowing for processing by screen printing and thus providing an alternative processing technique to the inkjet printing applicable for Electrolyte 1.

2.3 Electrochemical transistors

The base of the here investigated electrochemical transistors (ECTs) is the variable conductivity of PEDOT. As described in chapter 2.1.2 PEDOT is acting as an insulator in its neutral undoped state and as a conductor in its oxidised doped state. The switching between those two states is performed by a reversible redox reaction in the course of electrochemical doping. For this process two material components are needed: First a conductive polymer, in our case PEDOT:PSS, and second an electrolyte containing moveable cations and corresponding anions. Because the electrochemical doping and de-doping is a reversible process where the polymer is not damaged [35] it is possible to switch the PEDOT repeatedly between its two conductive states. In this way the ECTs are switched on and off. The chemical reaction proceeding in the course of this electrochemical doping and de-doping can be described by the redox reaction depicted in equation 2.2. Here the reversible reaction between the oxidized $PEDOT^+$ with a cation M^+ from the electrolyte and an electron e^- resulting in the formation of the neutral $PEDOT^0$ and the complex M^+:PSS^- is shown.

$$PEDOT^+:PSS^- + M^+ + e^- \leftrightarrow PEDOT^0 + M^+:PSS^- \qquad (2.2)$$

Roughly spoken, equation 2.2 describes the correlation between the conducting $PEDOT^+$ and the non-conducting $PEDOT^0$ and thus the fundamental function of an ECT. To understand the charge transport and the distribution of oxidized and reduced PEDOT inside the materials, being responsible for the obtained transistor behaviour of ECTs, two possible setups are described. These two setups - combining PEDOT:PSS and an electrolyte- are denoted as the dynamic configuration and the bi-stable configuration [31, 36]. Within both configurations equation 2.2 is valid.

The dynamic configuration [31, 36]

In the dynamic configuration one continuous line of PEDOT:PSS is covered with electrolyte (figure 2.12). When a negative voltage is applied at one side and the other side of the line is grounded, potential gradients along the line and between the PEDOT:PSS and the electrolyte are formed. These potential gradients lead to a series of redox reactions.

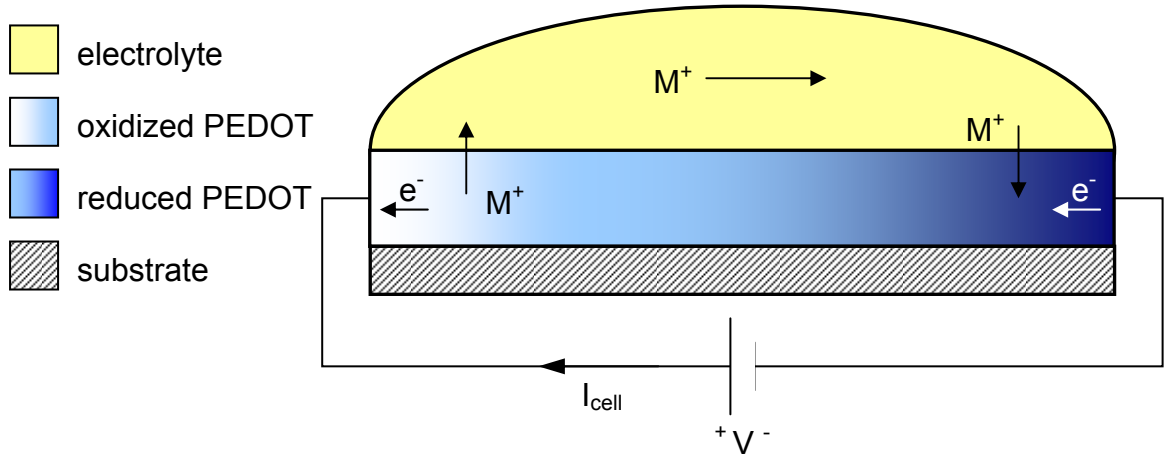

Figure 2.12: dynamic configuration combining PEDOT:PSS and an electrolyte

At the negatively biased side of the electrode reduction of the PEDOT:PSS will take place. When $PEDOT^+$:PSS^- is reduced, $PEDOT^0$ as well as PSS^- are formed. To maintain charge neutrality, either PSS^- has to migrate out of the polymer film into the electrolyte or a cation M^+ has to migrate into the film. Due to the high molecular weight of $PSS^-$and its long chains, PSS^- is not able to migrate out of the polymer film. Charge neutrality in the film is maintained by the M^+ cation migrating into the polymer film and forming M^+:PSS^-. Now this M^+ missing is leading to a charging of the electrolyte that needs to be balanced somewhere else along the PEDOT:PSS line. At the positively biased side of the line oxidation of the $PEDOT^0$ to $PEDOT^+$ takes place. Here the charge neutrality is maintained by M^+ cations migrating from the polymer film into the electrolyte because PSS^-, as mentioned before, is too big to migrate. Accordingly, the charge in the electrolyte, caused by the M^+ migrating into the polymer film at the negative biased side of the line, is balanced. These reactions lead to a redox state gradient of PEDOT from mainly reduced to mainly oxidised along the PEDOT:PSS line. This is depicted in figure 2.12 by the dark blue colour, representing reduced $PEDOT^0$, and by the white colour, representing oxidised $PEDOT^+$. The current in the dynamic structure is only transported by polarons as long as there is voltage applied. When the voltage is disconnected, the system goes back to its original stable state.

After description of the behaviour of the dynamic configuration at a constant voltage, its response to an increasing voltage V_D applied along the PEDOT:PSS line is discussed. At small voltages, the current I_D shows linear dependence on the voltage due to the homogeneously distributed impedance along the channel. When the

voltage is increased a condition is reached where the concentration of reduced and therefore non-conducting $PEDOT^0$ is so high that a saturation of the current is obtained. The point reaching this condition is called the pinch-off point. This is a result of the nonlinear decrease of the PEDOT:PSS conductivity with an increasing $PEDOT^0$ concentration at the negative biased side of the PEDOT:PSS line [37]. In figure 2.13 the response of the dynamic configuration to an increasingly applied voltage is depicted.

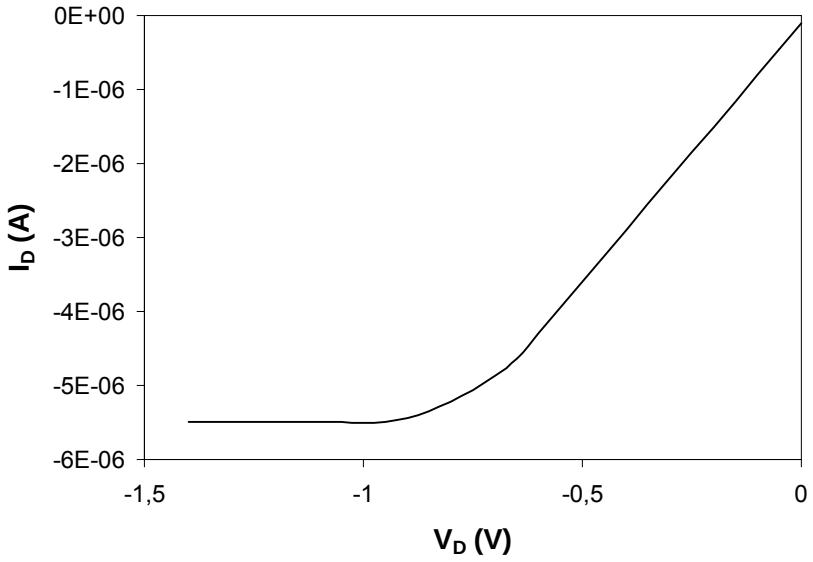

Figure 2.13: current response of the dynamic configuration to an applied voltage

The bi-stable configuration [31, 36]

In the bi-stable configuration two separated areas of PEDOT:PSS are observed. These two areas or electrodes are covered and connected by the electrolyte. In this way an electrochemical cell is created (see figure 2.14) where two electrodes of electron conducting material (PEDOT:PSS) are connected via an ion conducting material (electrolyte).

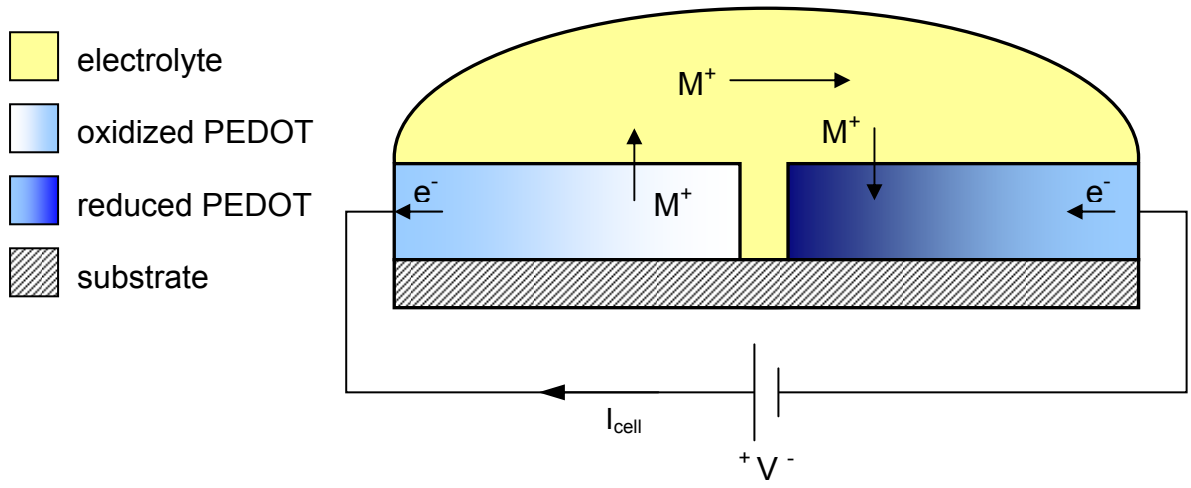

Figure 2.14: bi-stable configuration combining PEDOT:PSS and an electrolyte

When a voltage is applied reduction of the $PEDOT^+$:PSS^- to $PEDOT^0$ and PSS^- will occur at the negatively biased electrode. Additionally the cations M^+ are moving towards the negatively charged electrode. There they are migrating from the electrolyte into the polymer film to maintain charge neutrality. Because the two areas of $PEDOT^+$:PSS^- are connected to an electrochemical cell, the reduction at the negative biased electrode needs to be balanced by an oxidation at the positive charged electrode. Here the $PEDOT^0$ is oxidised to $PEDOT^+$. To maintain charge neutrality M^+ cations are migrating out of the polymer film into the electrolyte. The reduction and oxidation gradients in the electrodes depicted by the dark blue and the white colour as well as the moving of the cations are displayed in figure 2.14. As long as there is voltage applied, the electronic current is transferred into an ionic current by the versatile cations M^+ in the electrolyte and transported between the electrodes by moving M^+ cations. When the voltage is disconnected, the two electrodes stay in their redox states because the circuit of the electrolyte and the PEDOT:PSS is open. This is referred to a system showing bi-stability, giving the configuration its name. An application of the bi-stable setup is the electrochemical display which is based on the different colouring of oxidised and reduced PEDOT. Reduced $PEDOT^0$ shows a dark blue colour whereas oxidised $PEDOT^+$ is light grey which can be utilised to print a simple switchable bi-coloured display [7].

The layout of an electrochemical transistor can be seen as a combination of the two configurations described before. A possible setup to obtain a functional ECT,

consisting of PEDOT:PSS and an electrolyte, is shown in figure 2.15. The PEDOT:PSS is used for the electrodes, namely the source-drain line and the gate electrode. They are all located at the same level which allows for a straightforward processing by standard printing techniques. For comparison, in organic thin film transistors, the source, drain and gate electrodes are located in different layers, vertically separated by the gate dielectric thus resulting in at least four functional layers which complicates the printing process. The second active material, the electrolyte, is applied directly on top of the PEDOT:PSS electrodes ionically connecting the gate electrode and the source-drain line. With the assumption that there is no gate present, a cross section of the source-drain line can be described as the dynamic configuration. This cross section is marked in figure 2.15 as the cut A-A. Cut B-B, a cross section depicting a cut through the souce-drain line, the gate electrode and the region between them, all covered with electrolyte, can be described as the bi-stable configuration.

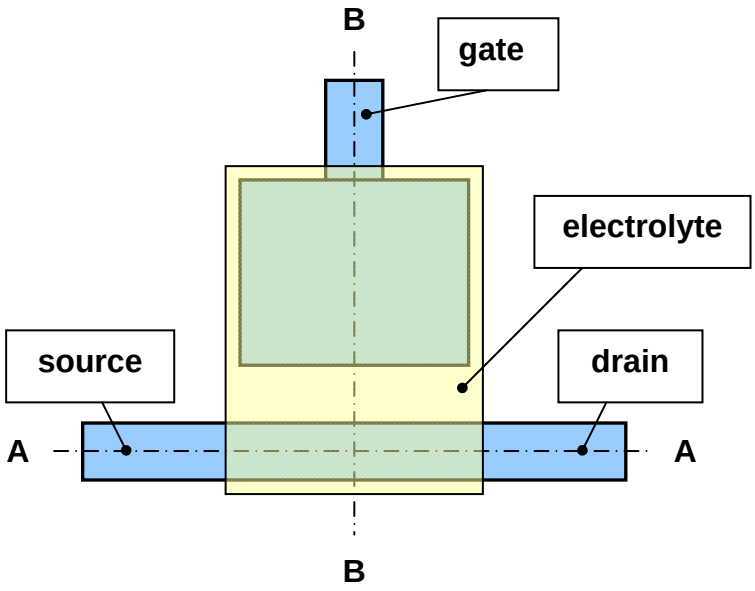

Figure 2.15: top view of an ECT depicting its basic design and the cuts A-A and B-B

To operate an ECT a voltage is applied to the source-drain line with the source being connected to ground. Thereby the redox states of the PEDOT in the source-drain line are affected and the impedance of the line is modulated. At the gate electrode a positive voltage is applied, interacting with the cations of the electrolyte and thereby modulating the impedance of the source-drain line. In this way an electrochemical device is fabricated that is a combination of the dynamic configuration and the bi-stable configuration described earlier. A generic set of characteristics when a positive

voltage V_g is applied to the gate and the potential at the drain V_D is varied is shown in figure 2.16.

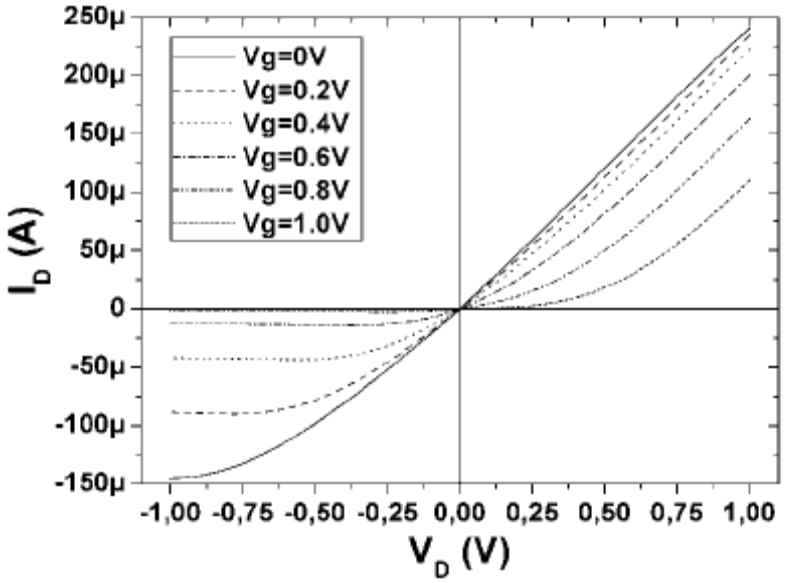

Figure 2.16: I(V) characteristics depicting the drain current response of an ECT to positive gate voltages V_g [31]

In the first quadrant in figure 2.16, where $V_g \geq 0$ V and $V_D > 0$ V, no transistor behaviour is obtained. When the gate voltage $V_g = 0$ V an oxidation at the drain side and reduction at the source side of the PEDOT:PSS line takes place. When a positive gate voltage is applied the source-drain line is reduced and the gate electrode is oxidized as long as the drain voltage V_D is low. With increasing positive V_D the potential in the source-drain line gets higher than the potential in the gate electrode. This leads to an oxidation of the source-drain line and a reduction of the gate electrode. In this way the conductivity of the source-drain line is increased, leading to an increasing drain current I_D with no chance for saturation behaviour. Because there is no transistor behaviour in this quadrant of the characteristics it is not practicable to operate a device in this quadrant.

Usually electrochemical transistors are operated in the third quadrant where $V_g \geq 0$ V and $V_D < 0$ V. As long as $V_g = V_D = 0$ V, the source-drain line is reduced and the gate electrode is oxidised. When V_D is increased, the device is showing the behaviour of the dynamic configuration and the drain current I_D is increasing until saturation. When V_g is increased, the gate electrodes potential is getting higher compared to the potential of the source-drain line, leading to an intensified reduction and thereby a

higher impedance of the source-drain line. This is depicted by a less steep slope of the output characteristic in its linear region and saturation at a lower I_D. According to equation 2.2 this results in an intensified oxidation of the gate electrode. This behaviour shows the interaction of the two configurations. The dynamic configuration describes the redox gradient and the saturation of the current when no V_g is applied and the bi-stable configuration describes how this transistor behaviour is influenced by a positive gate potential V_g tuning the redox reaction of the whole electrochemical device.

The used materials and the behaviour of the electrochemical transistors involve some rules concerning the design and manufacturing. First of all it is crucial for the functionality that there is no electrical connection between the gate and the source-drain line because the functionality is dependent on the combination of electronic and ion conducting materials. Moreover the ratio between the gate electrode area A_G and the area of the source-drain line covered with electrolyte A_{SD} is very important (figure 2.17). Since the used PEDOT:PSS ink consists of only 20% undoped $PEDOT^0$ in its pristine state, the gate electrode area needs to be at least 5 times larger then the area of the source-drain line covered with electrolyte to match the amount of reducable $PEDOT^+$ with the amount of oxidisable $PEDOT^0$. By D. Nilsson it is suggested that the gate area should be at least 10 times the active area on the source-drain line to provide enough $PEDOT^0$ that can be oxidised to guarantee a sufficient reduction of the source-drain line without the risk of over-oxidation [31]. Over-oxidation is an irreversible oxidation process resulting in permanently damaged PEDOT:PSS [38, 39]. In addition, the resistance of the source-drain line in the linear regime of the I(V) curve is affected by the area ratio between the gate area and the active area on the source-drain line leading to an increasing resistance with increasing area ratio [31]. Since the performance of the electrochemical transistors is significantly influenced by this area ratio it is important to consider the area ratio when planning ECTs. In chapter 4.1.3 the influence of other geometry parameters on the device performance is described.

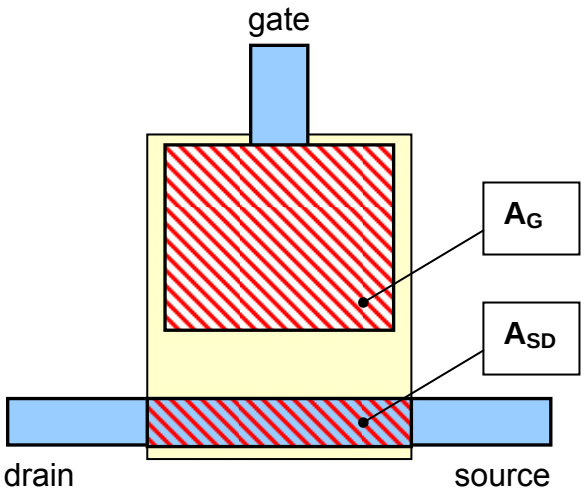

Figure 2.17: top view of an ECT depicting the gate electrode area A_G and the active area on the source-drain line A_{SD}

2.4 Electrochemical inverters

An inverter, also called a NOT Gate, is an element in digital logic which implements logical negation: when the input is 0 the output is 1 and vice versa. A possibility to realize such an element in organic electronic is the organic complementary inverter. This inverter consists of a p-type and an n-type transistor. The gates as well as the drains of the two transistors are connected to each other and the source of the p-type transistor is connected to the supply voltage V_{Sup} (see figure 2.18 a)).

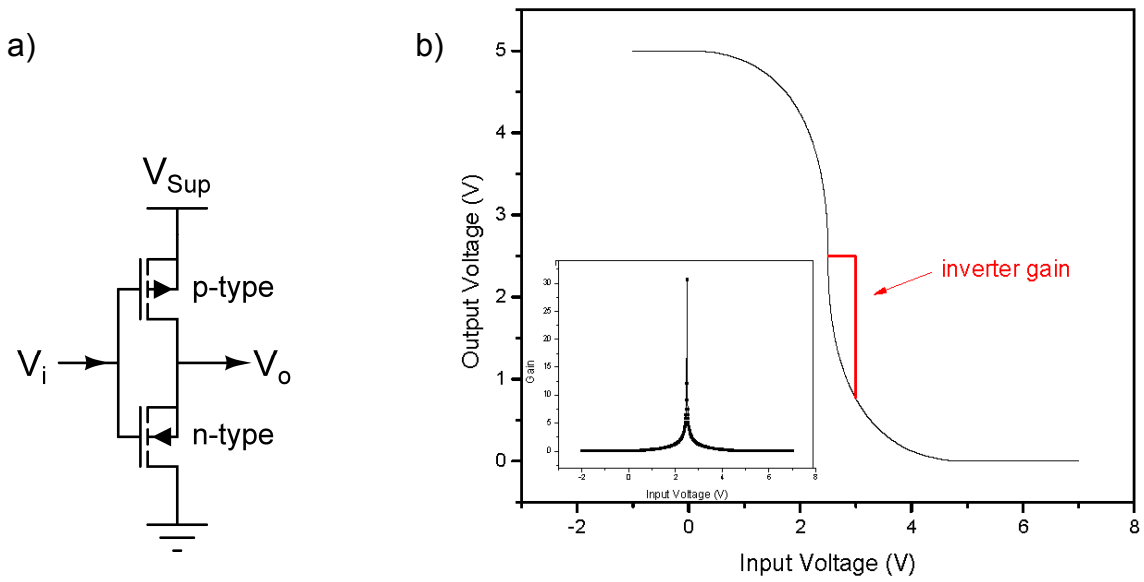

Figure 2.18: a) circuit scheme of an organic complementary inverter b) transfer characteristic of an inverter inset: gain of an inverter [40]

The combined gate acts as the input signal and the combined drain as the output signal. When the inverter is in one of the logic states, one of the transistors is off and the other one is on, the output voltage is either zero or equal to the supply voltage. An idealized transfer characteristic depicting this switching behaviour is shown in figure 2.18 b). The highest slope of the transfer curve is representing the gain which is an important parameter of the inverter (inset figure 2.18 b)). The higher the gain, the smaller is the input voltage region where the inverter is neither in the high nor in the low logic state. In organic complementary inverters the gain depends on the time where both transistors are on while switching one transistor on and the other one off. In contrast, electrochemical inverters use only one transistor. Thus the gain of the electrochemical inverter depends on the characteristic of this one transistor,

determining its switching behaviour. The electrochemical transistors that are the base for the electrochemical inverters operate in the third quadrant of the set of characteristics as depicted in chapter 2.3 figure 2.16. As a consequence it is not possible to switch one transistor with the output voltage of another one. To make those transistors accessible for the use in logic circuits the output signal needs to be shifted from a negative to a positive voltage. This is achieved by a voltage divider that is connected to the drain electrode of the transistor. As proposed by Nilsson et al. [41] the voltage divider consists of three consecutive resistors R_1, R_2 and R_3 and two supply voltages V_{DD} and $-V_{DD}$ at the ends of the resistor chain. The input of the inverter V_{in} is the gate electrode of the transistor that is connected to the voltage divider between the resistors R_2 and R_3. The output of the inverter V_{out} is between the resistors R_1 and R_2 (compare figure 2.19).

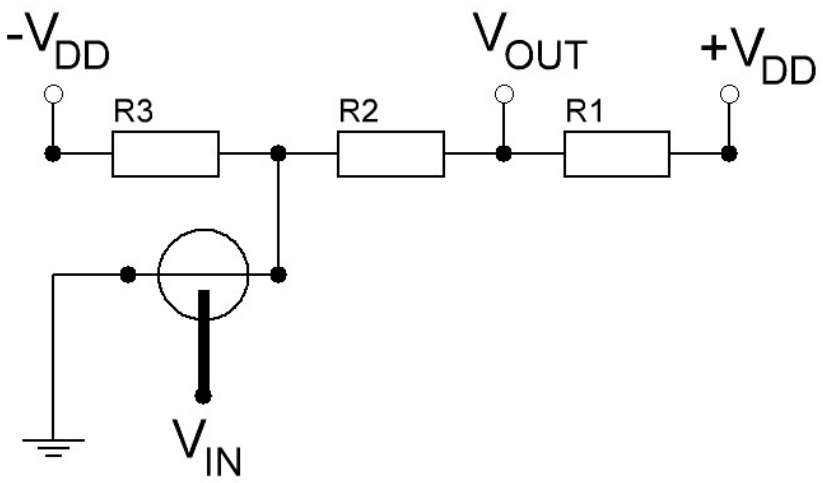

Figure 2.19: circuit diagram of an electrochemical inverter

A combination of an electrochemical transistor and the attached voltage divider is working as an inverter where a signal at the gate of the transistor of logic 0, representing a voltage of zero volts, is transferred into an output signal of logic 1, representing a positive voltage at the output of the voltage divider. An input signal of logic 1, representing a positive voltage that is large enough to switch off the transistor, is transferred into an output signal of logic 0. In this way a signal inverting behaviour is achieved.

To calculate the output voltage V_{out} when the resistors of the voltage divider are known (or vice versa) the ECT is substituted by a resistor. This resistor has two limit states. When the transisor is switched on, this resistor reaches its minimum value, further on referred to as R_{ON}. Its maximum value, called R_{OFF}, is reached by this resistor when the transistor is switched off. Comparing this resistor to R_3 of the voltage divider, two idealized cases -representing the limit states of the inverter- can be assumed. The following two assumptions have to be made to achieve this idealized behaviour.

In the first case, when a logic 1 is applied to V_{in}, it is assumed that R_{OFF} of the switched off transistor exceeds the resistance of R_3 so much that R_{OFF} can be neglected and the circuit shown in figure 2.20 a) is valid. In this case V_{out} depends only on the three resistors of the voltage divider and the supply voltages. This dependency, rooted in the voltage divider theory, is shown in equation 2.3. By changing the equation the resistors can be calculated too (equation 2.4).

$$V_{out} = \frac{V_{DD} - (-V_{DD})}{R_1 + R_2 + R_3} \cdot (R_2 + R_3) \tag{2.3}$$

$$R_2 + R_3 = \frac{R_1}{(V_{DD} - (-V_{DD})) - V_{out}} \cdot V_{out} \tag{2.4}$$

The second case, when a logic 0 is applied, R_{ON} of the switched on transistor is assumed to be so much smaller than R_3 that R_3 is negligible, resulting in the circuit shown in figure 2.20 b). Here V_{out} depends on the resistors R_1 and R_2 of the voltage divider, the resistance R_{ON} of the switched on transistor and the positive supply voltage V_{DD} (see equation 2.5). The resistors can be calculated by equation 2.6.

$$V_{out} = \frac{V_{DD}}{R_1 + R_2 + R_{ON}} \cdot (R_2 + R_{ON}) \tag{2.5}$$

$$R_2 + R_{ON} = \frac{R_1}{V_{DD} - V_{out}} \cdot V_{out} \tag{2.6}$$

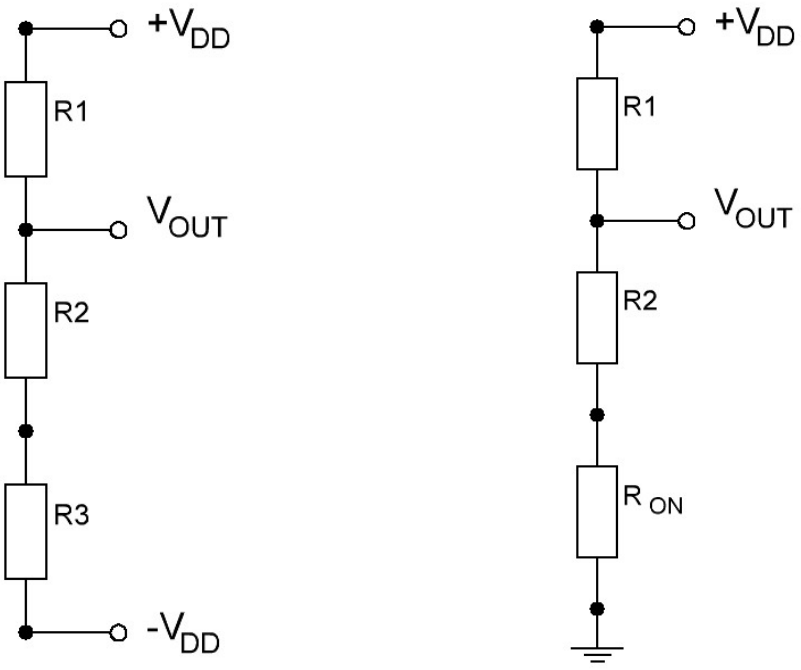

Figure 2.20: a) circuit diagram if $R_{OFF} >> R_3$ b) circuit diagram if $R_{on} << R_3$

Contrary to the idealized cases R_{OFF} is not infinitely high in reality when the transistor is switched off and R_{ON} is not so much smaller than R_3 when the transistor is switched on that R_3 can be neglected. So both resistors, R_3 and R_{ON} respectively R_{OFF}, have an influence on the output voltage V_{out} when the transistor is switched on and off. To calculate V_{out} with both resistors taken into account, the “Helmholtz´sche Überlagerungssatz” is used. Both “ideal” cases discussed before are combined to one circuit (figure 2.21). Then two different calculations are performed, shortcutting first the voltage source V_{Gr} (Case A, figure 2.22) and second the voltage source V_{DD} (Case B, figure 2.23) and calculating all the voltages in the circuit. These two cases have to be calculated for the switched on transistor with the resistance R_{ON} and the switched off transistor with the resistance R_{OFF}. So these two resistances are referred to as R_E in the following.

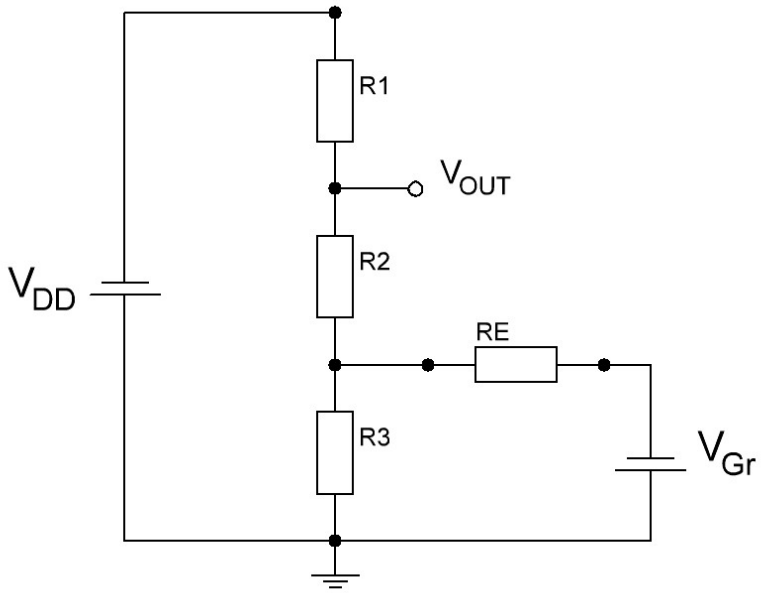

Figure 2.21: circuit diagram of the combined circuit according to the "Helmholtz´sche Überlagerungssatz"

Case A

From voltage divider theory the equation to calculate V_{out} is derived (equation 2.7). The output voltage is calculated by the relation of the combined resistors R_p and R_2 to the sum of all resistors.

$$V_{out} = \frac{R_2 + R_P}{R_1 + R_2 + R_P} \cdot V_{DD} \tag{2.7}$$

The resistor R_P in equation 2.7, combining the parallel resistors R_3 and R_E, is calculated with equation 2.8.

$$R_P = \frac{R_3 \cdot R_E}{R_3 + R_E} \tag{2.8}$$

The sum of the output voltage V_{out} and the voltage across the resistor R_1, $V_{1,A}$, has to be the same as the supply voltage V_{DD}. Thus V_{1A} can be calculated by equation 2.9.

$$V_{1,A} = V_{DD} - V_{out} \tag{2.9}$$

The current across the two resistors R_1 and R_2 is the same because they are connected in series, so the voltage across R_2, V_2, can be calculated by equation 2.10.

$$V_2 = \frac{V_{1,A} \cdot R_2}{R_1} \tag{2.10}$$

Across the two parallel connected resistors the voltage is the same. It is defined by the supply voltage minus V_1 and V_2 (equation 2.11) since $V_{1,A}$, V_2 and V_3 need to fit the supply voltage V_{DD}.

$$V_E = V_3 = V_{DD} - V_{1,A} - V_2 \tag{2.11}$$

With V_E and V_3 calculated all the voltages in the equivalent circuit diagram of case A according to the “Helmholtz´scher Überlagerungssatz” are defined.

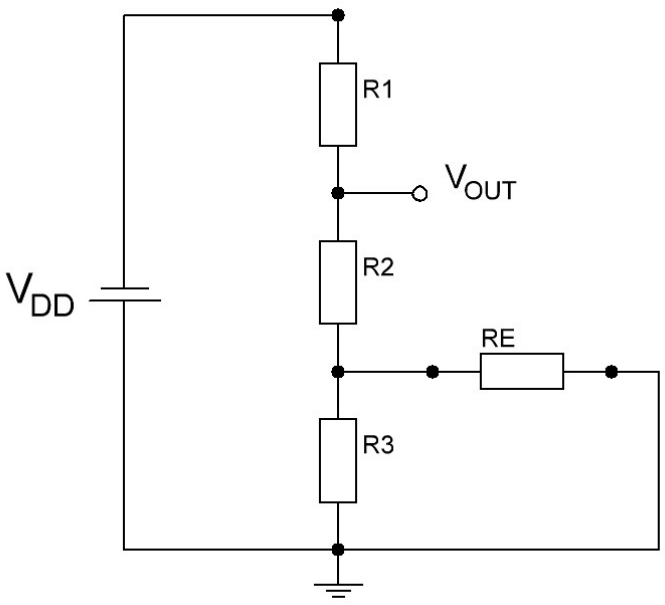

Figure 2.22: circuit diagram of the case A circuit according to the “Helmholtz´sche Überlagerungssatz”

Case B

The output voltage V_{out} is calculated by the relation of the combined resistor R_P to the sum of all resistors (equation 2.12).

$$V_{out} = \frac{R_P}{R_E + R_P} \cdot V_{Gr} \tag{2.12}$$

To calculate the resistor R_P, the sum of the resistors R_1 and R_2 is combined with the parallel connected resistor R_3 using the standard formula for parallel resistors. The resulting equation is shown as equation 2.13.

$$R_P = \frac{R_3 \cdot (R_1 + R_2)}{R_3 + R_1 + R_2} \tag{2.13}$$

Due to the fact that the sum of V_E and V_{out} results in the second supply voltage V_{Gr}, V_E can be calculated as shown in equation 2.14. V_3 and V_E also have to sum up to V_{Gr}, so V_3 can be calculated with equation 2.15.

$$V_E = V_{Gr} - V_{out} \tag{2.14}$$

$$V_3 = V_{Gr} - V_E \tag{2.15}$$

Because R_1 and R_2 form a voltage divider on their own with V_{out} as their supply voltage, the formula for voltage dividers can be used to calculate $V_{1,B}$ (equation 2.16). In this sub voltage divider the sum of $V_{1,B}$ and V_2 has to yield V_{out}, so V_2 can be calculated by equation 2.17.

$$V_{1,B} = \frac{V_{out}}{R_2 + R_1} \cdot R_1 \tag{2.16}$$

$$V_2 = V_{out} - V_{1,B} \tag{2.17}$$

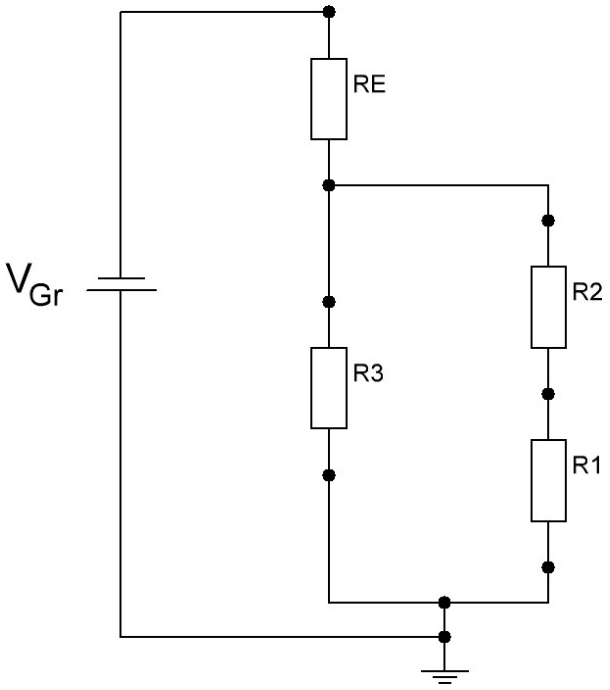

Figure 2.23: circuit diagram of the case B circuit according to the “Helmholtz´sche Überlagerungssatz”

By combining $V_{1,A}$ and $V_{1,B}$ of these two cases (see equation 2.18), an output voltage $V_{out,\ combined}$ for the system considering R_3 and R_E and thus providing a more realistic value for the output voltage can be calculated with equation 2.19.

$$V_{1,combined} = V_{1,A} - V_{1,B} \tag{2.18}$$

$$V_{out,combined} = V_{DD} - V_{1,combined} \tag{2.19}$$

As shown above, the output voltage V_{out} is determined by the resistors and the supply voltages. To achieve a requested output voltage, the resistance and the ratio of the resistors as well as the supply voltages need to be tuned. The supply voltages are suggested by Nilsson et al. [41] for this voltage divider suitable for electrochemical transistors, but the resistors need to be adapted for the used transistors. As depicted by the idealized cases, the resistor R_3 has to be in the range between R_{ON} and R_{OFF}. This is a precondition for the functionality of the electrochemical inverter. With the R_{ON} / R_{OFF} values known from the on-current and the off-current of the used transistor, the value for R_3 can be determined. Considering the value of R_3 it is

possible to calculate the other two resistors by the equations 2.4 and 2.6 and complete the voltage divider for the electrochemical transistors in this way.

3 Experimental

3.1 Electrolyte fabrication

For this work two electrolytes with completely different compositions are used.
Electrolyte 1 is a polyelectrolyte like described in chapter 2.2.2. The formulation is nearly identical to an electrolyte that has already been used for electrochemical devices [42]. The composition showing mass fraction and aggregate state of the different constituents is depicted in table 3.1.

Table 3.1 composition of Electrolyte 1

Component	Aggregate state	Mass fraction [%]
Deionised water	liquid	51
Glycerol (85wt%)	liquid	8
D-sorbitol	solid	8
Poly(sodium-4-styrene sulfonate)	solid	33

The components are processed as follows

- Mixing of water and glycerol, mechanical agitation (magnetic stirrer) until a homogenous blend is achieved
- Adding of D-Sorbitol, mechanical agitation until complete dissolution
- Adding of Poly(sodium-4-styrene sulfonate) (PSS:Na), due to the high mass fraction of the PSS:Na it should be added in three portions, first manual agitation is needed until a suspension is formed followed by mechanical agitation

During the last step a lot of bubbles are formed. They disappear with time and a clear yellow solution with a quite low viscosity is obtained.

Electrolyte 2 is a polymer electrolyte (see chapter 2.2.3). It is a milky white paste with a quite high viscosity. The composition and fabrication protocol are confidential and cannot be disclosed in this work.

3.2 Inkjet printing

For the inkjet-printing the Dimatix® Materials Printer DMP 2800, which is shown in figure 3.1, is used. It is an easy to use and effective precision materials deposition system. Its possible applications are generation of samples, development of products, development and evaluation of materials and fluids as well as the evaluation of interactions between a certain fluid and substrate combination [43]. It has also been used to fabricate inkjet-printed sensors that utilize PEDOT:PSS electrodes [8]. Main advantages despite the easy handling and the efficiency are the low operating temperature, the capability to print on flexible substrates and high printing rates which would make inkjet-printing suitable for mass production. Also, the loss of active material is reduced to a minimum because, in contrast to spin coating and following etching processes, ink jet printing is an additive printing process where only the amount of material is applied that is actually required.

Figure 3.1 : Dimatix® DMP-2800 inkjet printer [44]

The used inkjet printer allows the deposition of fluidic materials on an A4 format substrate with a thickness of up to 25 mm. During printing, the substrate is secured in place by the vacuum platen. The applied vacuum is not only fixing the substrate it also gives the opportunity to print on flexible substrates because it flattens the substrate on the platen surface. Another feature of the platen is the adjustable temperature. It is possible to heat it up to a maximum temperature of 60 °C. On the whole platen area this printer can create and define patterns. This variety is offered by employing a pattern editor program [43]. With this program sizes, line widths, distances and, via the possibility to adjust the number of layers printed on top of each

other, also the thickness of samples can be predefined. In addition to predefining the printing pattern the resolution of the printing can be adjusted in the pattern editor program. This is done by adjusting the space between two drops that are printed next to each other. This is varying the resolution in x direction. In y direction this is done by adjusting the head angle of the print head and thereby changing the distance of to printed drops in y direction.

Another feature of this printing system is the fiducial camera. In figure 3.2 a view through this camera is shown. This camera allows for positioning of the print origin to match previously printed structures or otherwise patterned substrate, provides measurement of already printed features and locations on the sample and gives the opportunity for inspecting and taking pictures of printed patterns or drops [43].

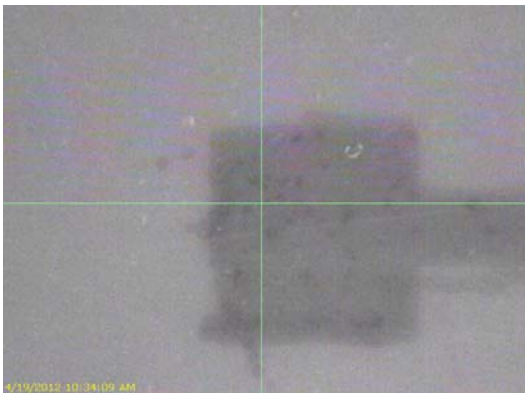

Figure 3.2 view through fiducial camera

There is a second camera existing on the printing system. It is a dropdown camera system to monitor the shape of the drops fired by the piezo-electric drop casting system included in the head of the printing cartridge that is shown in figure 3.3.

Figure 3.3: printing cartridge [45]

This print head is a MEMS-based (Micro-Electro-Mechanical-Systems) cartridge-style print head that can be filled by the user with its own inks. Each cartridge has a capacity of 1.5 ml. To enable printing of a series of different fluids without removing

the substrate and shut down the printing system, the cartridges can be easily replaced. Each print head has 16 nozzles useable for dropcasting that are evenly distributed over a length of 254 microns with typical dropsizes of 10 pico liters [43]. A piezo crystal located at every nozzle is used to control the drop properties. The factor that controls the piezo crystal and thereby the drop size and volume is the so-called firing voltage. During the process of drop formation the firing voltage is controlled by the wave form. In the following this process is described [44].

The typical basic waveform is divided into four segments that are shown in figure 3.4. The Start or Standby position of the piezo is shown in figure 3.4 a). At this position the fluid chamber is depressed. The next phase is the firing pulse phase shown in figure 3.4 b). Here the piezo is brought back to a neutral relaxed position by decreasing the firing voltage to zero volts. At this point the chamber has its maximum volume and the fluid is pulled into the chamber. Also the fluid meniscus at the nozzle is pulled in. In figure 3.4 c) the drop ejection phase is depicted. Here the chamber is compressed by increasing the firing voltage and thereby deform the piezo. This leads to the ejection of a drop. The final phase is the recovery phase shown in figure 3.4 d). The piezo voltage is decreased and the chamber decompresses in preparation for the next pulse.

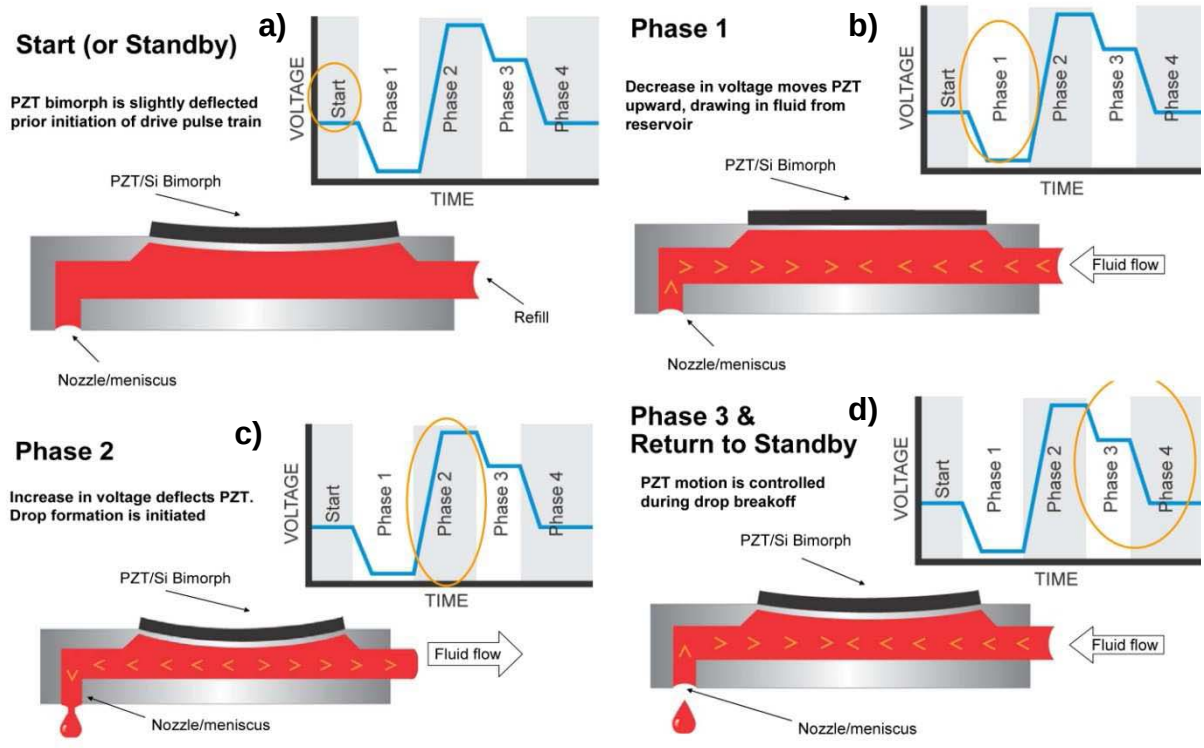

Figure 3.4: four phases of the basic drop casting waveform a) start phase b) firing pulse phase c) drop ejection phase d) recovery phase [44]

Each of the four phases of has three properties: duration, voltage level and slew rate. By adjusting these properties the drop size and shape and its tear-off behavior can be controlled. Figure 3.5 shows ink drops in the process of tearing off from the print head nozzles recorded by the dropdown camera system.

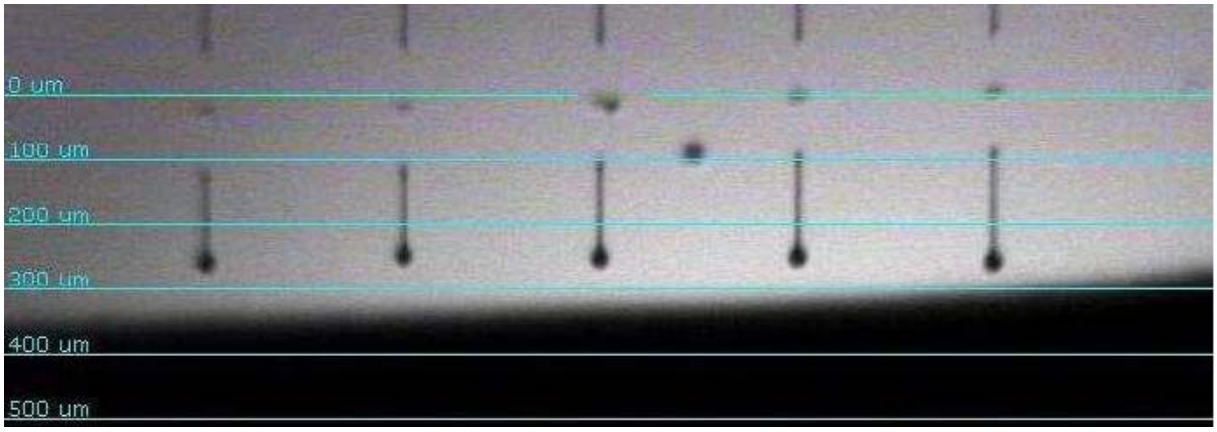

Figure 3.5: view through dropdown camera showing tearing off ink drops

There are some specifications the inks must fulfill to be printed with the dimatix printing cartridges. The first is a viscosity less than 30 mPa·s, but 10 to 12 mPa·s would be the optimal range for defined drops and high enough drop velocities. The second is a low evaporation rate. If the evaporation rate is too high, the ink will dry at the nozzle to air interface. Also particles included in the inks should not be bigger than 0,2 µm, which is a hundredth of the size of the nozzle diameter, and should not agglomerate or settle rapidly [46]. These limitations must be kept in mind when planning manufacturing processes based on inkjet-printing.

3.3 Spin coating

Spin coating is a common way to fabricate thin films on plane substrates. To achieve such thin films a liquid precursor with a polarity that is fitting the properties of the substrate surface is needed. Also the viscosity and the surface tension of the liquid precursor, called resist from now on, are critical parameters influencing the homogenity and thickness of the achieved film. A few drops of the resist are applied on the center of the substrate which is than rotated with 1000 to 6000 rpm. The resist is moved towards the edges of the substrate by the occuring centrifugal forces and thereby formes a continuous layer. Excess resist flows off the edges and is desposed into the waste reservoir of the spin coater. Additionally to the resist properties, the acceleration and the rotating speed and time are crutial for the obtained layer thickness and homogenity.

All spin coating processes in this work are performed using a Laurell® WS-650S-6NPP/Lite Spin-coater that is depicted in figure 3.6 in clean room conditions.

Figure 3.6: Laurell® WS-650S-6NPP/Lite Spin-coater [47]

3.4 Device preparation

The samples described in this work where fabricated via two different pathways. In figure 3.7 pathway **A**, the manufacturing process where some process steps are carried out by hand, is shown. Pathway **B** in figure 3.7 shows the device fabrication of entirely inkjet printed electrochemical transistors and inverters. Both processes are carried out under ambient conditions at room temperature.

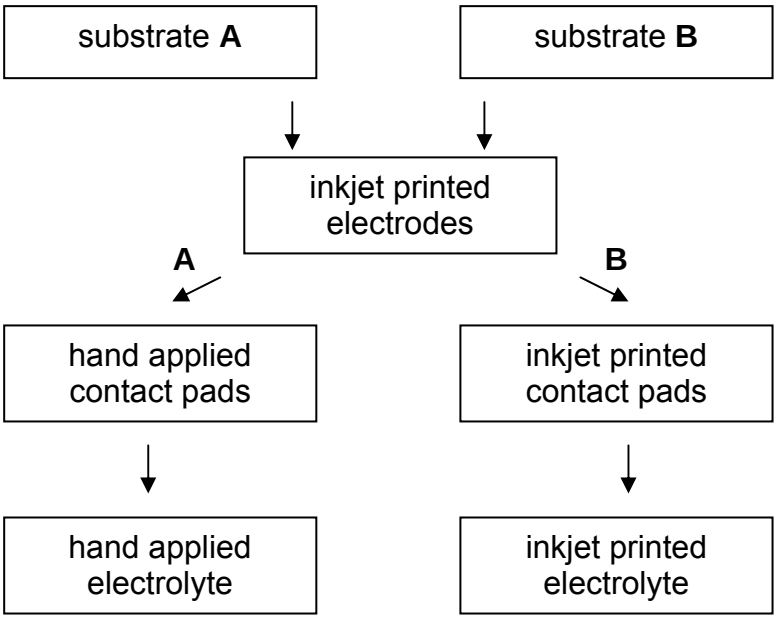

Figure 3.7: device preparation pathways

3.4.1 Device preparation by hand (pathway A)

To proof the functionality of the electrochemical transistors based on our materials and fabricated with our PEDOT:PSS process, some process steps are carried out by hand.

Polyethyleneterephthalat substrate A

As a substrate Melinex ST504 from DuPont® is used. This is a polyethylenterephthalat (PET) foil that is crystal clear, heat stabilized and pretreated on one side to promote adhesion [48]. The substrate is used without any cleaning steps or other preparations.

PEDOT:PSS electrodes

In this fabrication pathway the electrodes are the only components of the devices that are fabricated by inkjet-printing. The PEDOT:PSS used is Clevios P Jet HC from H.C.Stark®. It is a water based solution with organic solvents and binders. The viscosity is up to 20 mPa·s, the conductivity is between 30 and 90 S/cm. The blue colored ink has a pH-value of 1,5 to 2,5 and a solid content between 0,6 and 1 % [49]. The Inkjet printer and the process of inkjet printing are described in chapter 3.2.

Silver contact pads

To improve the electrical contact between the PEDOT:PSS electrodes and the probing needles of the MB® Parameter analyzer (see Chapter 3.5.4) silver contact pads are applied at the ends of the electrodes. Electrolube® silver conductive paint is used. It is a grey liquid that dries in about 10 minutes at room temperature and then provides a thin, smooth film with a sheet resistance of 0.01 to 0.03 Ohms/sq [50]. The silver is gently applied by hand using a wooden tooth pick and dried under ambient conditions.

Electrolyte

The electrolyte, in combination with the PEDOT:PSS electrodes, bears the functionality of the whole device. It is prepared as described in chapter 3.1 and is, similar to the silver ink for the contact pads, gently applied by hand. One drop of undiluted electrolyte is applied to ensure the functionality of the devices.

3.4.2 Device fabrication by inkjet-printing (pathway B)

The following is a description of the manufacturing steps carried out to fabricate electrochemical transistors and inverters based on those transistors. The manufacturing process is shown in figure 3.7 pathway **B**. All steps are performed by inkjet printing. The used inkjet printer and the inkjet printing process are described in chapter 3.2.

PET substrate B

The substrate used for those devices is a Melinex ST725 PET foil from DuPont® that is cut into handy pieces. It is a high clarity polyester film that is pretreated on both sides to promote adhesion to many industrial coatings and inks [51]. A thin foil to

protect the substrate surface is removed directly before the substrate is put into the inkjet-printer. This ensures that the surface remains protected from damage and pollution until the manufacturing process starts. No further preparation of the foil surface is performed. The only exceptions are the transistors described in chapter 4.2.1. There a layer of microresist® UVcur06 [52] is spun on with a spin speed of 3000 rpm and 30 seconds spinning time. It is cured for 90 seconds with UV-light under vacuum.

PEDOT:PSS electrodes

For the electrodes the printable PEDOT:PSS solution Clevios P Jet HC from H.C.Stark® is used.

The ink is filled into the cartridge with a syringe and filtered through a 0,2 µm PET filter to prevent a clogging of the print head nozzles. Then the cartridge is mounted onto the inkjet-printer. The basic settings of the printing are summarized in the following table 3.2.

Table 3.2 basic settings of PEDOT:PSS printing

Substrate temperature [°C]	Firing voltage [V]	Drop length [µm]	Drop spacing [µm]	Print head angle [°]
40	22-25	300-350	20	4,5

After the printing the sample is placed on a heat plate for 15 minutes at a temperature of 100°C to remove the remaining solvent from the printed material. A picture of PEDOT:PSS electrodes fabricated by inkjet-printing with the settings described above is shown in figure 3.8.

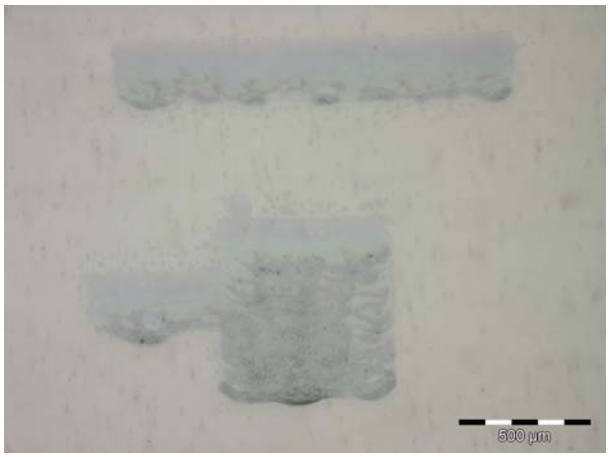

Figure 3.8: printed PEDOT:PSS

Silver contact pads

The contact pads are prepared from a cabot® corporation silver ink named CCI-300. This is an inkjet-printable ink with ethanol and ethylene glycol as the main solvents

containing silver nano particles. The viscosity of the grey-green liquid is in the range of 11 to 15 mPas. 19 to 21 % of the silver ink is solid silver in the form of nano particles [53].

To distribute the silver particles homogenously the ink is put into a ultrasonic bath for 15 minutes before it is filtered with a 0,2 µm PET filter and filled into the cartridge of the printer. The settings of the inkjet-printer are summarized in table 3.3.

Table 3.3 basic settings of silver ink printing

Substrate temperature [°C]	Firing voltage [V]	Drop length [µm]	Drop spacing [µm]	Print head angle [°]
40	30-33	450-500	10	2,3

When the printing of the contact pads is finalized, the sample is put on a heat plate for 30 minutes at a temperature of 100°C. This removes the solvent and the silver nano particles are sintered together to provide a continuous metal conductor with a very low resistivity. A picture of printed contact pads on the PEDOT:PSS electrodes is shown in figure 3.9.

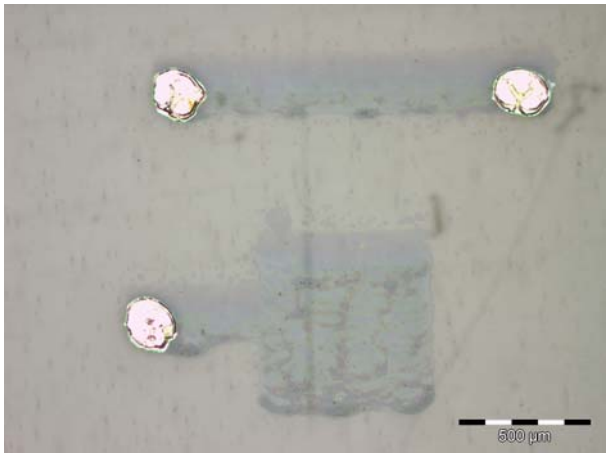

Figure 3.9: printed silver ink

Electrolyte

Due to the very high viscosity of Electrolyte 2 only Electrolyte 1 is used for application by inkjet-printing. Although the viscosity is quite low, Electrolyte 1 still needs to be diluted with deionized water in the volume ratio of one part electrolyte and three parts water (1 + 3). After this dilution the electrolyte is liquid enough to be printed with well defined drops and without too much sprinkling. The diluted electrolyte is filtered with a 0,2 µm PET filter, filled into a printer cartridge and than is ready for printing. In contrary to the PEDOT:PSS and the silver 20 layers of electrolyte have to be printed to achieve the desired functionality of the devices. For further information on the electrolyte dilution and the need for 20 printed layers see chapter 4.2.

The main printer setting is shown in table 3.4. Additionally to those settings a cleaning step of the cartridge nozzles after every printed layer of electrolyte is performed.

Table 3.4 basic settings of electrolyte printing

Substrate temperature [°C]	Firing voltage [V]	Drop length [µm]	Drop spacing [µm]	Print head angle [°]
RT	25-27	350-400	20	4,5

After printing the electrolyte the device is completed (figure 3.10) and can be electrically characterized. For further information on the electrical characterisation see chapter 3.5.4 and for results of those measurements see chapter 4ff.

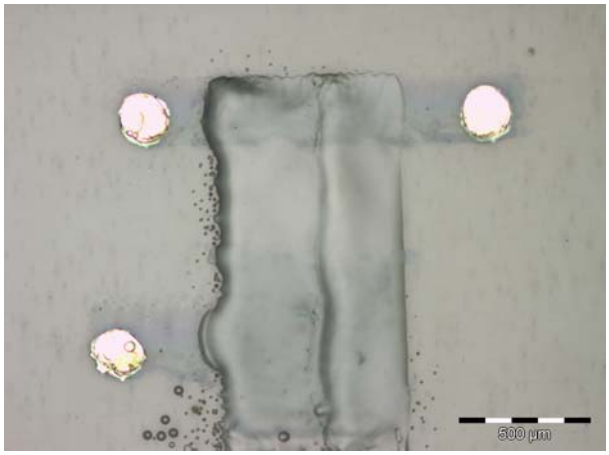

Figure 3.10: printed electrolyte

3.5 Device characterization

3.5.1 Optical microscope

Optical microscopy is one of the standard methods for examining samples since the invention of microscopes back in the 17th century. It is used in every scientific field where samples that are too small to be resolved by the human eye have to be investigated.

In optical microscopy visible light and a system of lenses is used to produce a magnificated view of the sample. Basically the lens system consists of an objective lens with a very short focal length that works like a magnifying glass and an eyepiece with a couplet of two lenses. In the eyepiece a virtual image is created by the first lens. The second lens enables the eye to focus on this virtual image. A picture of the optical path is shown in figure 3.11. The overall magnification is the product of the magnifications of the objective lens and the eyepiece. The limit of magnification is reached when it is impossible to resolve separate points. This is known as the resolution limit d (see equation 3.1). It is defined by the wavelength of light λ and the numerical aperture (NA) of the objective lens. Common microscopes have a resolution limit of about 200 nm.

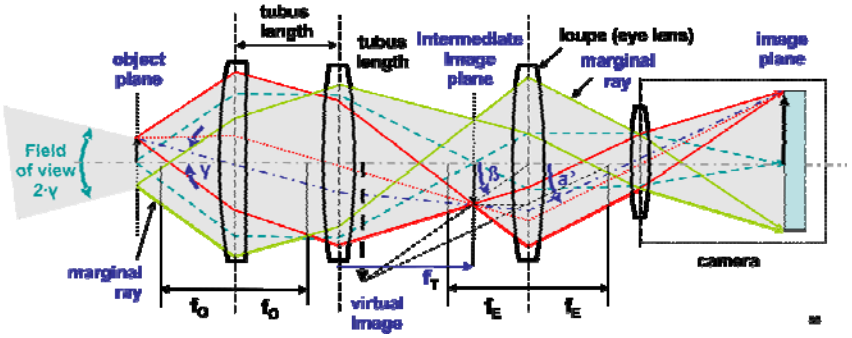

Figure 3.11: optical path of a microscope [54]

$$d = \frac{\lambda}{2NA} \tag{3.1}$$

An Olympus® BX51 microscope with magnifications between 5 and 100 is used to examine the prepared samples. Also an Olympus® digital camera together with software called “analysis work image processing” is used to take digital pictures,

adjust their brightness and contrast settings and add measuring beams. All the microscope pictures shown in this work are recorded with the components mentioned before.

3.5.2 Four point prober

The four point probes method is widely used for resistivity measurements of thin films of conductors and semiconductors.

The advantage of this measurement is its setup that eliminates the impedance contribution of the wiring and contact resistances. To achieve this, two separated pairs of electrodes, with the known distance s between each other, are used. These electrodes are arranged linearly as shown in figure 3.12 a). A current is supplied via the outer pair of electrodes (A). This generates a voltage drop across the sample. But there is also a voltage drop in the wiring and at the contacts of this pair of electrodes. If these electrodes would be used to measure the resistance of the sample surface, these factors would lead to an error in the result. To exclude these interfering factors and only measure the voltage drop across the sample surface, the inner pair of electrodes (B) is used. This pair of electrodes is connected to a high impedance voltmeter. Almost no current flows through the inner electrodes (B) leading to a very low voltage drop in the wiring and as a result to a very small interfering factor. With this setup of current supplying electrodes and separated voltage tapping electrodes a very accurate measurement of the samples resistivity is achieved.

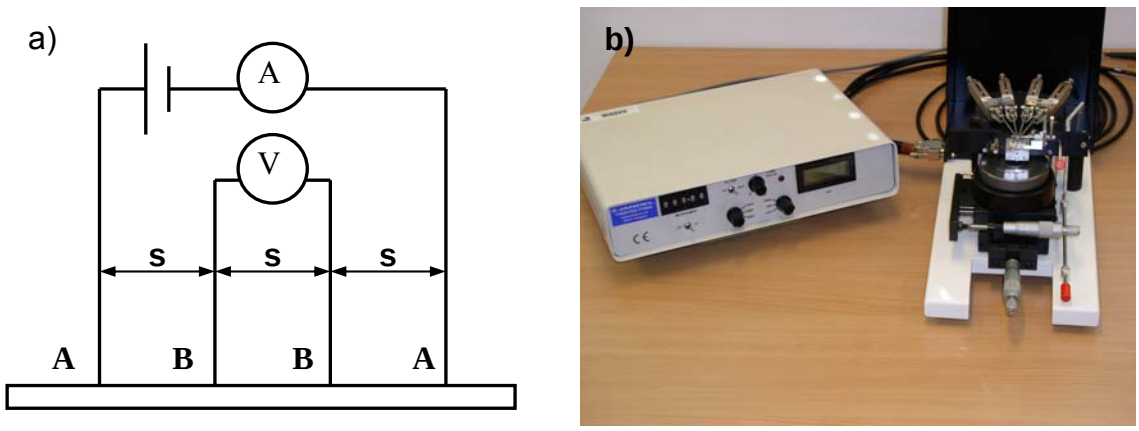

Figure 3.12: a) scheme of the 4 point probes measurement b) Jandel® 4 point prober

Knowing the supplied current and measuring the voltage, the sheet resistance Rs can be calculated using the following equation (3.2).

$$R_s = f \cdot \frac{U}{I} \tag{3.2}$$

The factor f in this equation is the correction factor suitable for samples with a thickness below 40% of the distance between the electrodes s and a measurement that is carried out at a distance from the sample edge that is at least 4 times s [55]. For the limitations mentioned before this factor f is π / ln (2) or 4,532. To set the sheet resistance apart from the bulk resistance, the unit of the sheet resistance is defined to be Ohm per square, although it is also calculated from voltage divided by current.
To characterize the PEDOT:PSS samples a Jandel® 4 point prober (see figure 3.12 b)) with tungsten electrodes and a distance between the electrodes s of 0,1 cm is used. A current of 0,1 mV is applied and the voltage is measured. The sheet resistance is calculated using equation 3.2.

3.5.3 Surface profiler

The Surface profiler measurement is a very common measuring method to determine the thickness of thin films and the roughness of surfaces on a macroscopic scale, contrary to AFM which delivers micro-roughness values. There are three different types of surface profilers: optical, contact and pseudo-contact method profilers. In this work only the contact method surface profiler was used and is described more closely.
The contact mode profiler uses a diamond tipped stylus to scan over the sample surface that is mechanically coupled to the core of a linear variable differential transformer (LVDT) [56]. It is first moved vertically until it touches the sample and then moved laterally across the surface. The procedure of scanning is shown in figure 3.13 a). The moving speed (v_m) is determined by the scan time and the scan length. Both factors can be preset by the control software. Also the force of the stylus applying on the sample surface can be controlled. These settings, as well as the radius of the stylus tip, affect the achievable resolution. During the movement of the stylus the surface irregularities, depicted by the vertical deviation of the stylus Δh, are recorded. This is achieved by generating electrical signals corresponding to the stylus movement as the core position of the LVDT changes. With this position change an AC referance signal is scaled that afterwards is converted to a digital signal

through an integrating analog to digital converter. By recording this signal as a function of the position a profile of the sample surface is displayed.

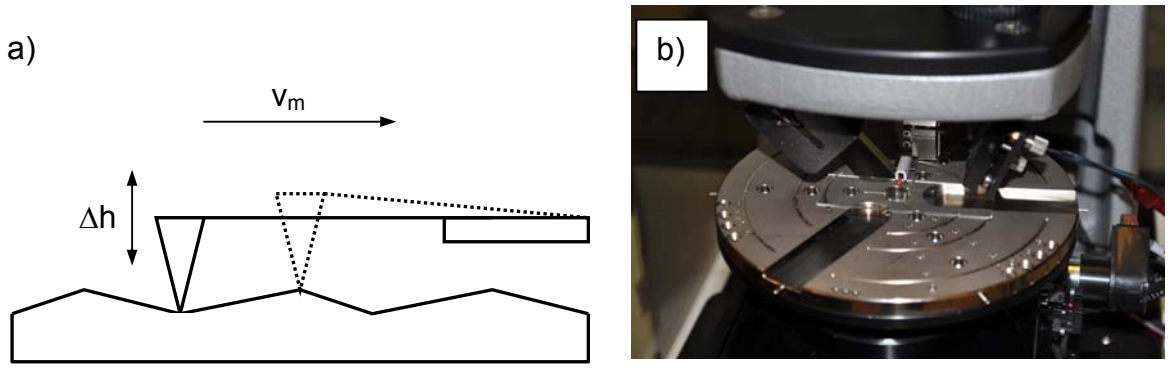

Figure 3.13: a) scheme of surface profiler scanning procedure b) measuring unit of Veeco® Dektak 150 surface profiler

For the measurements carried out in this work a Veeco® Dektak 150 surface profiler is used (figure 3.13 b)). The used scanning parameters are a scanning rate of 20 micrometers per second and a tracking force of 5 milligrams. For all measurements a stylus with a tip radius of 12,5 micrometers is used.

3.5.4 Electrical measurements

To verify the functionality and the performance of the built transistors and inverters (see chapter 3.4) they need to be characterized by electrical measurements. To fulfill that task a measuring setup is used that already has been used to characterize organic thin film transistors and inverters [57] (figure 3.14).

The samples are contacted on a probe station using probes from Suess Microtec®. The actual measuring is performed with a MB Technologies® parameter analyzer. The parameter analyzer is equipped with four source measuring units (SMU). All measuring parameters are controlled by the corresponding operating software that also depicts the processes and results of the measurement.

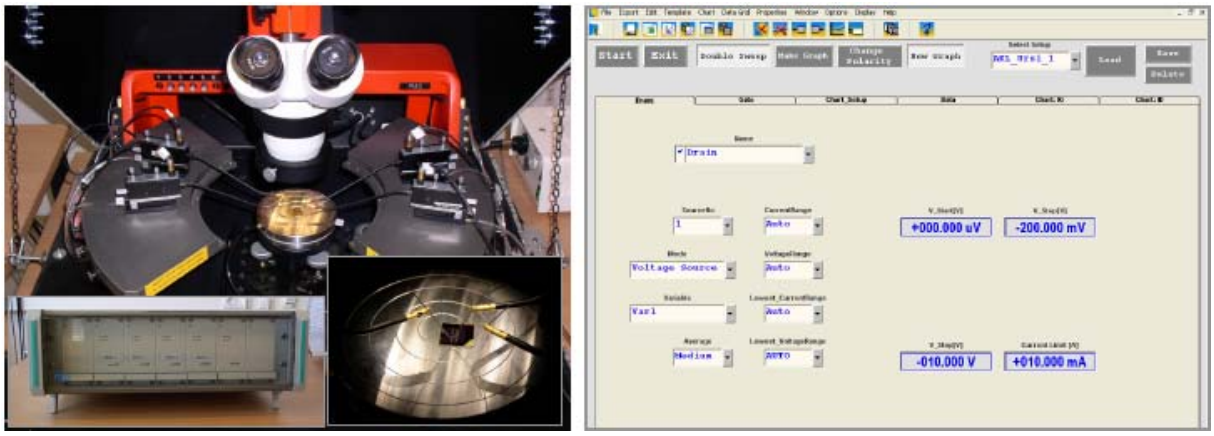

Figure 3.14: measuring setup for the electrical characterisation of ECTs and inverters [57]

For the electrical characterization of the different devices different measuring setups are required that are explained in the following.

Electrochemical transistors

The main parameter to characterize the electrochemical transistors is the output characteristic. For that purpose three SMUs have to be connected to the contacts of the ECT shown in figure 3.15. On the gate electrode a voltage V_g between 0 V and +1 V increasing in 0,25 V steps is applied. The drain voltage V_D is increased from 0 V to –1 V with a 0,05 V step width and the source is grounded. The resulting source-drain I_D current is recorded to determine the output characteristics of the transistor.

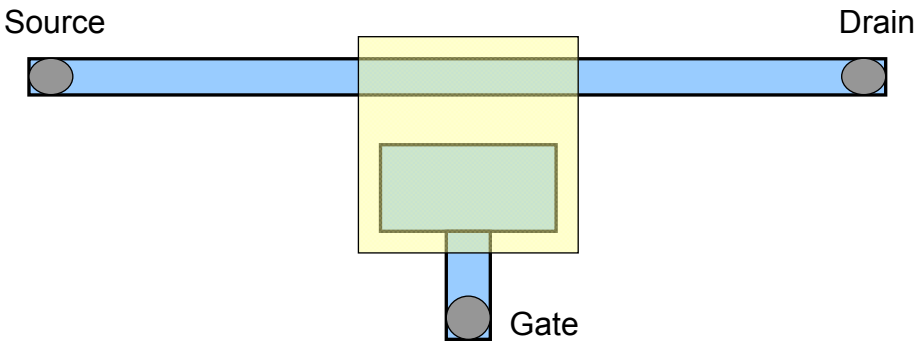

Figure 3.15: contact scheme of an ECT

Inverters based on electrochemical transistors

To record the inverter characteristics five probes are needed. They are connected as shown in figure 3.16. On the $+V_{DD}$ contact a voltage of +3 V and on the $-V_{DD}$ contact a voltage of –3 V is applied. On the gate electrode, which is the input, a voltage V_{in}

increasing from 0 V to +1 V in 0,05 V steps is applied. The drain electrode is grounded and at V_{out} the resulting voltage is measured.

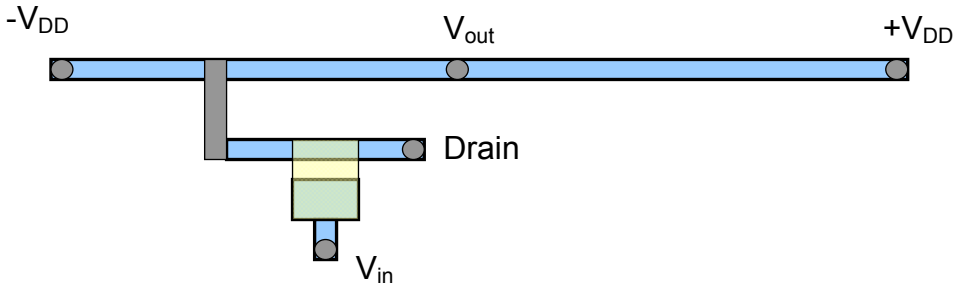

Figure 3.16: contact scheme of an inverter

For dynamic measurements of the inverters a slight modification of the measurement setup has to be performed. The input signal is no longer generated by the MB Technologies® parameter analyzer but is supplied by a Thurlby Thandar Instruments® TG230 frequency generator. Also the output signal is separated from the parameter analyzer and is connected to a Tektronix® TDS 2014 B oscilloscope where the outcoming voltage is recorded. All other contacts remain unchanged. A circuit diagram of the new measuring setup is shown in figure 3.17. The data from the oscilloscope is processed with the Tektronix® Open Choice Desktop analyzing software

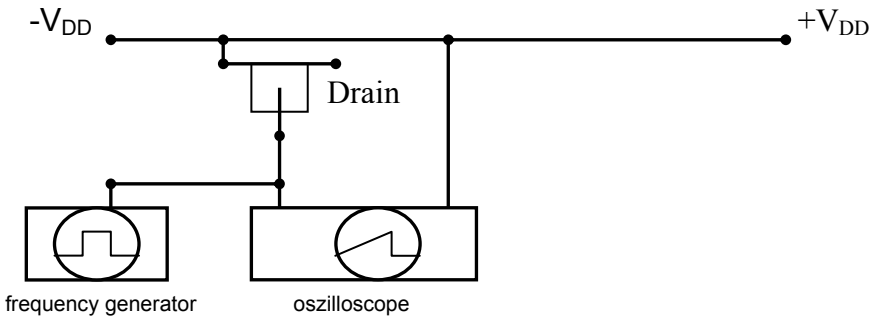

Figure 3.17: circuit diagram of the measuring setup for dynamic measurements

For the dynamic measurements $+V_{DD}$ and $-V_{DD}$ remain at +3 V and –3 V respectively. The drain is grounded. The square wave input signal V_{in} switches between 0 V and +1 V with a frequency of 0,05 Hz.

The results of the electrical measurements of transistors and inverters are discussed in chapter 4ff.

4 Results and Discussion

4.1 ECTs with electrolyte applied by hand

4.1.1 First ECTs with printed electrodes

The first electrochemical transistors are fabricated to confirm the functionality of devices using inkjet printed PEDOT:PSS as electrodes. Also the possibility to use Electrolyte 1 and Electrolyte 2 (see chapter 2.2.7) in combination with the inkjet printed PEDOT:PSS is evaluated. To achieve this, electrodes are printed according to the rules for designing electrochemical transistors described in chapter 2.3. Since these devices should only show that the combination of inkjet printed PEDOT:PSS and Electrolyte 1 or 2 result in functional transistors, the electrolyte, as well as the silver contact pads, are applied by hand. The resulting transistors are electrically characterised afterwards. A transistor using Electrolyte 1 is shown in figure 4.1 a). For the depicted transistor a resulting output characteristic as well as the gate switching current are shown in figure 4.1 b) and c).

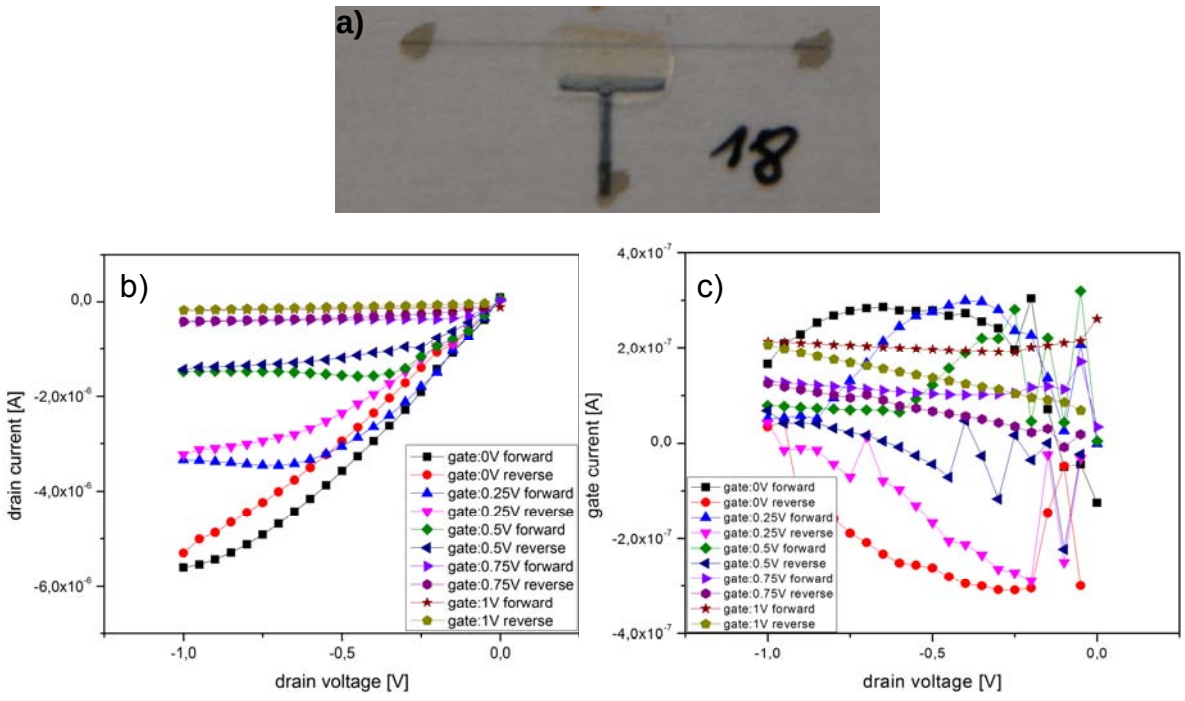

Figure 4.1: a) photograph of a transistor with a source-drain line width of 350 µm, a gap between the gate electrode and the source-drain line of 1500 µm and an area ratio between the gate electrode and the active area on the source-drain line of 10:1 b) output characteristic c) gate switching current

The obtained output characteristics show transistor behaviour. Saturation is visible although it is less pronounced at a gate voltage of V_g = 0 V. The output characteristic shows a maximum hysteresis of $h_{max} = 6{,}7 \cdot 10^{-7}$ A at a gate voltage of V_g = 0 V that is a result of the ions that have to be moved during the switching process. Their mobility is slow (compared to the mobility of the charge carriers in the channel) thus resulting in a hysteresis between forward and reverse sweep recorded at practicable (= not ultraslow) measurement times. These ions are responsible for the reduction of the PEDOT:PSS and are driven by the electric field between the gate and the active area on the source-drain line. The movement of the ions result in a gate switching current between the gate and the source-drain line (figure 4.1 c)) that is unavoidable for this type of transistors. Because the shape of the characteristic is quite similar and the range of the gate switching current is within one order of magnitude for all ECTs fabricated in this work, this characteristic is shown only for the first transistors. The on-current at a gate voltage of V_g = 0 V and a source-drain voltage of V_D = -1 V is $I_{on} = -4{,}6 \cdot 10^{-6}$ A. The off-current I_{off} at a gate voltage of V_g = 1 V and a source-drain voltage of V_D = -1 V is $I_{off} = -1{,}8 \cdot 10^{-7}$ A. The on/off ratio is 55. This on/off ratio as well as all following on/off ratios is calculated by dividing the on-current I_{on} through the off-current I_{off}. Compared to transistors from literature the on/off ratio is low [6]. In comparison to the transistors shown in the following chapters the on/off ratio is low too. A reason for this may be the used substrate. The PET foil used for these transistors was stored at ambient conditions for a long time. In this way a layer of humidity can be formed on the foils surface influencing the electrochemical behaviour of the PEDOT:PSS. Additionally the surface showed scratches and other inhomogeneities leading to defects in the printed PEDOT:PSS lines. With those interference factors known, the use of this substrate can be avoided leading to an improvement of the on/off ratios. Although the performance of these first ECTs is not very satisfying, the functionality of the devices is confirmed with these obtained results.

4.1.2 Comparison of different electrolytes

After the usability of the inkjet printed PEDOT:PSS has been confirmed the performance of the two available electrolytes is compared. The electrolytes differ in many attributes. The first variation is the type of the contained anion. Electrolyte 1 uses polyanions while Electrolyte 2 uses single anions. Additionally, different cations are used to drive the reaction. Regarding the physical properties the differing

viscositiy is the most prominent distinguishing characteristic making them suitable for different manufacturing processes. Electrolyte 1 with the lower viscosity is proper for inkjet printing while Electrolyte 2 with the higher viscosity is suitable for screen printing. Because there are plenty of differences between the two electrolytes, both in the formulation and the possible processing, electrical characterisations to determine the performance in combination with the inkjet printed PEDOT:PSS are executed. To be able to compare the measurements two transistors with similar dimensions are used. At one transistor Electrolyte 1 and at the other one Electrolyte 2 is applied. The output characteristics of these devices are shown in figure 4.2.

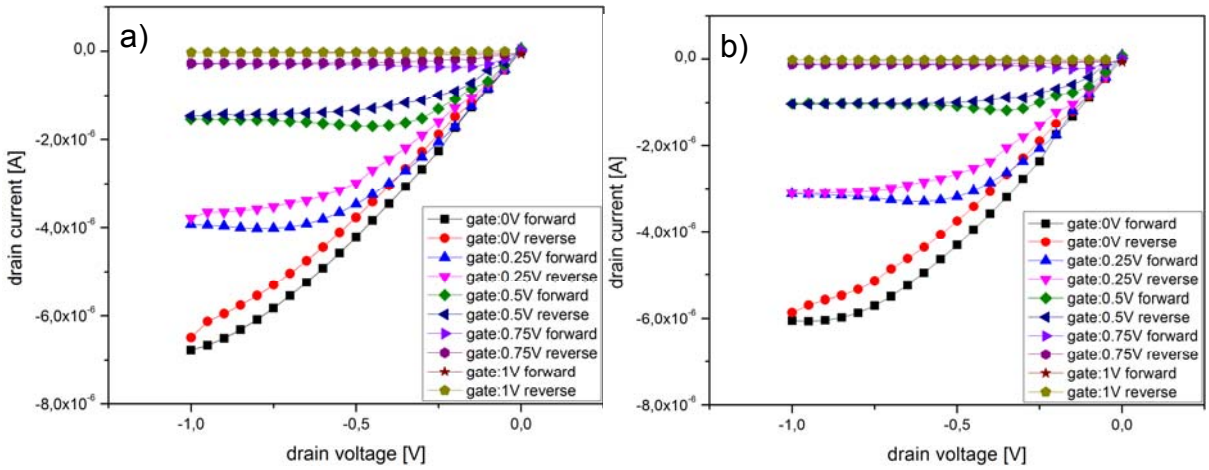

Figure 4.2: output characteristic of an ECT with a source-drain line width of 250 µm, a gap between the gate and the source-drain line of 1000 µm and an area ratio between the gate and the active area on the source-drain line of 10:1 using a) Electrolyte 1 and b) Electrolyte 2

The output characteristics shown in figure 4.2 a) belong to a device build with Electrolyte 1. There is hardly any difference to the output characteristics of a transistor using Electrolyte 2, shown in figure 4.2 b), noticeable except for the saturation that is less pronounced when using Electrolyte 1. Both transistors show maximum hysteresis h_{max} at a gate voltage of V_g = 0 V in a similar range. For the device using Electrolyte 1 $h_{max} = 5{,}6 \cdot 10^{-7}$ A and for the device using Electrolyte 2 $h_{max} = 6{,}2 \cdot 10^{-7}$ A. Also the variation of the on/off ratio is small, 252 for Electrolyte 1 and 260 for Electrolyte 2. The on-current is $I_{on} = -6{,}8 \cdot 10^{-6}$ A for Electrolyte 1 and $I_{on} = -6{,}0 \cdot 10^{-6}$ A for Electrolyte 2. The off-current is $I_{off} = -2{,}7 \cdot 10^{-8}$ A for Electrolyte 1 and $I_{off} = -2{,}3 \cdot 10^{-8}$ A for Electrolyte 2. Even though the electrolytes contain different anions and diverse cations are used to drive the reaction, their performance is very similar. In contrast to the performance the possible processing techniques are significantly

different. Electrolyte 1 on the one hand is well suited for inkjet printing applications while Electrolyte 2 on the other hand is usable for screen printing. In summery it can be claimed, that two electrolytes with nearly similar performance but differing processing possibilities are provided with Electrolyte 1 and Electrolyte 2.

4.1.3 Influence of different transistor geometries

With the functionality of the devices confirmed and the performance of the electrolytes compared, the influence of different transistor geometries on their performance is evaluated. Not only the electrolyte, but also the geometry and the dimensions of the device influence the performance of the electrochemical transistor. That is why these examinations are necessary. They are performed using transistors with the designs shown in figure 4.3 a). All the dimensions are chosen in accordance to the rules for designing transistors mentioned in chapter 2.3 and are given in millimeters. While varying different dimensions of the devices, the ratio between the gate area and the active area of the source-drain line of 10:1 remains unchanged The reason for this is the influence of this area ratio on the device performance, especially the on/off ratio, that should be excluded from the measuring series to focus on the influence of the varying dimensions. These varied dimensions are the thickness of the PEDOT:PSS electrodes T and the gap between the gate electrode and the source-drain line G. These variations were performed using transistors with different line widths of the source-drain line W represented by the different designs (figure 4.3 a)). A sketch depicting the varied dimensions is shown in figure 4.3 b).

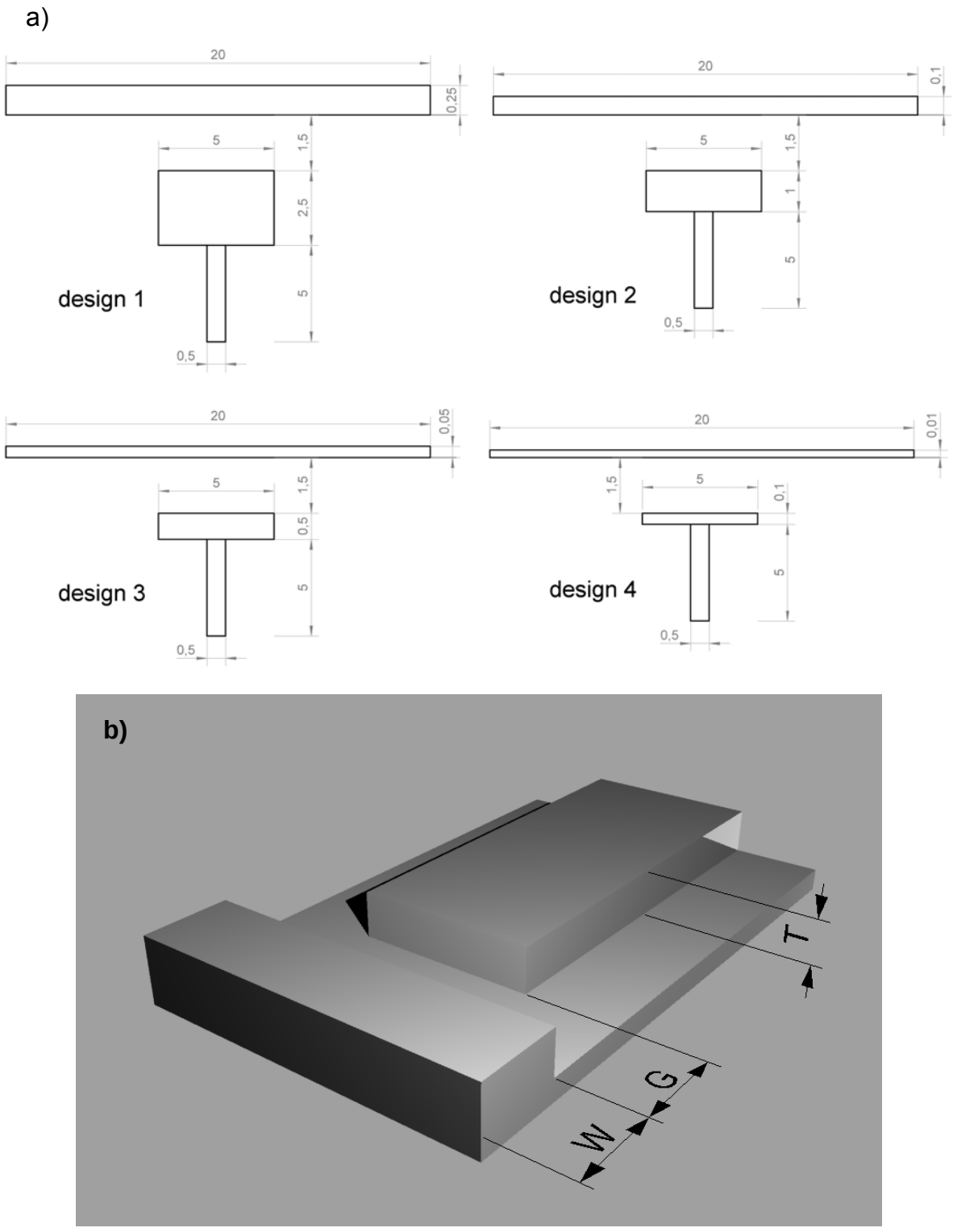

Figure 4.3: a) sketch of different transistor designs b) visualization of the varied dimensions

Variation of the electrode thickness

For this evaluation all different designs (1 to 4) shown in figure 4.3 a) are used. To obtain different thicknesses of the gate electrode and the source-drain line the number of PEDOT:PSS layers printed on top of each other by the inkjet printer is increased. First the influence of the varying thickness on the sheet resistance of the

PEDOT:PSS is investigated and afterwards the change of the transistor performance caused by this variation is examined. After printing, the line thicknesses are measured using a surface profiler. This procedure is described in chapter 3.5.3. Profiles of PEDOT:PSS lines with a nominal line width of 50 µm with a different amount of layers printed are shown in figure 4.4. The line thicknesses are read off considering the shape of the profiles with the edges thicker than the middle of the lines.

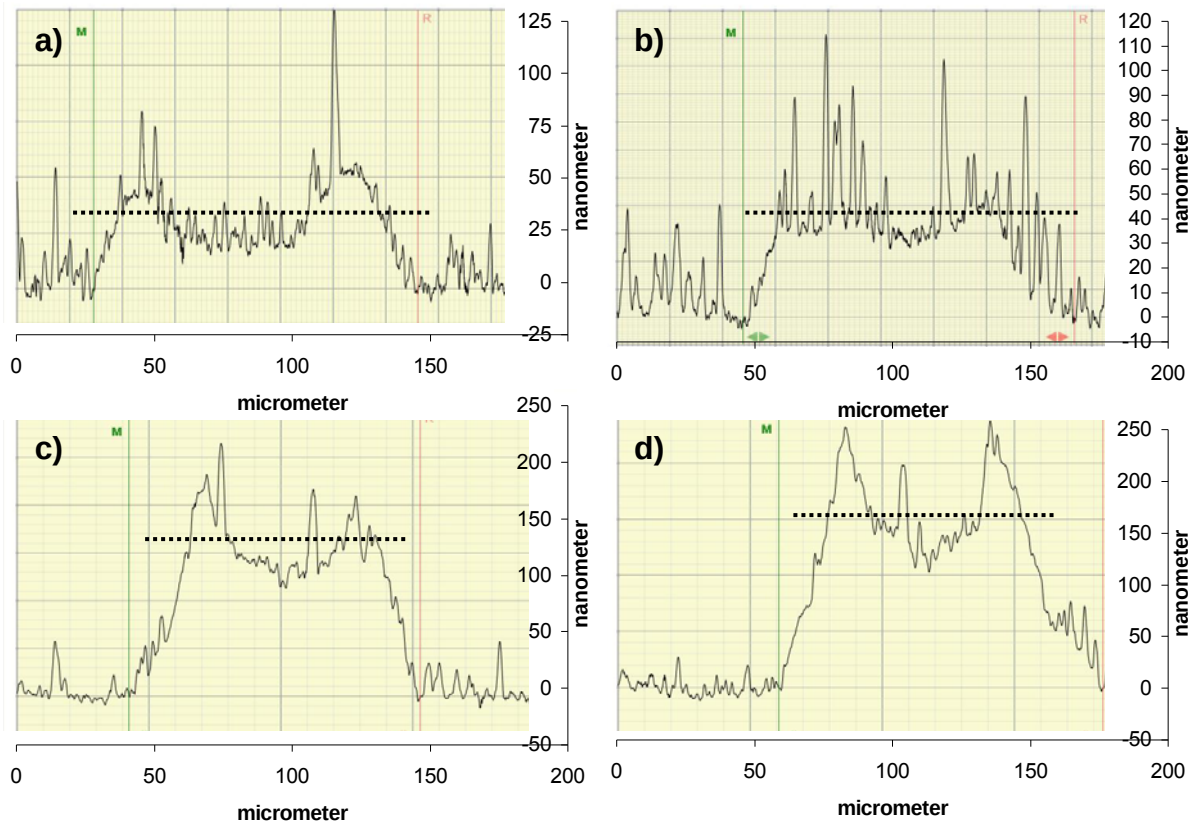

Figure 4.4: surface profile of a PEDOT:PSS line with different amount of layers printed and the read off thickness values depicted by the dashed lines a) one printed layer b) two printed layers c) three printed layers d) five printed layers

In the depicted profiles a higher thickness on the edges of the printed PEDOT:PSS lines is visible independent from the numer of printed layers. This is a result of the coffee ring effect. For a single drop this effect is explained in literature by a capillary flow induced by the differential evaporation rates across the drop. The liquid evaporating from the edge is replenished by liquid from the interior. The resulting edgeward flow can carry the majority of the dispersed material to the edge [59]. Transfering this knowledge to the printing of lines this flow is present perpendicular to

the printing direction and thereby leads to the bulges at the edges of the lines, clearly visible in figure 4.4.

Varying the thickness of the electrodes is expected to influence the electrical resistance. In order to study this change four point probe measurements are carried out (see chapter 3.5.2) and the sheet resistence corresponding to the thickness of the PEDOT:PSS is calculated with equation 3.2. The resulting sheet resistance curve is shown in figure 4.5.

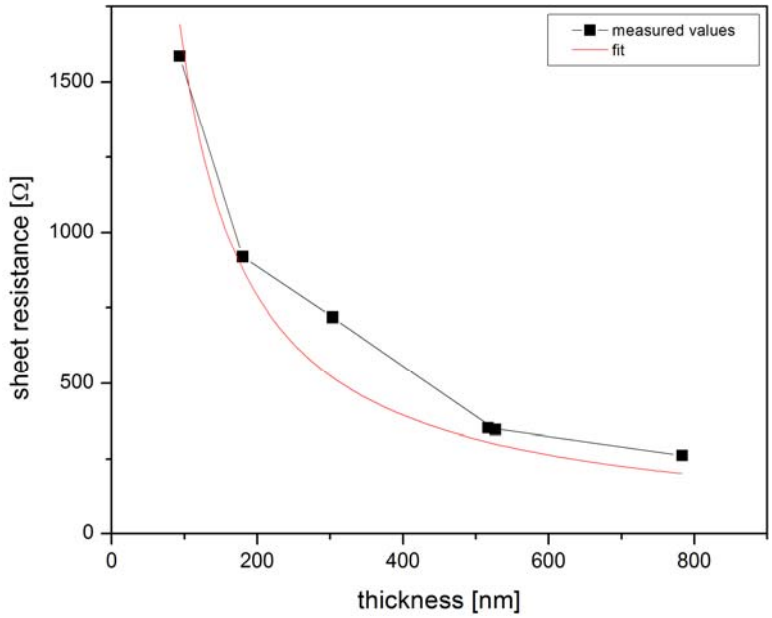

Figure 4.5: sheet resistance depending on PEDOT:PSS thickness

As depicted the sheet resistance is decreasing with increasing line thickness of the PEDOT:PSS. This corresponds to an increasing conductivity with increasing line thickness, which is the expected result. Also the trend of the curve is quite simmilar to a trend from literature depicting the sheet resistance of PEDOT:PSS depending on its thickness. In figure 4.5 a trend of $y = a \cdot x^{-1}$ is depicted, corresponding with the trend obtained in literature [60]. Considering the measured sheet resistance at a thickness of 100 nm the expected current for a voltage of one volt is in the range of 10^{-4} A. This in general is an entirely sufficient current in organic electronics where currents of 10^{-6} A are common. It is also an evidence that there is no need for PEDOT:PSS thicknesses larger then 100 nm to obtain an adequate current.

After the investigations of the varying thickness on the basic properties of the PEDOT:PSS, the influence on the device performance is measured. Electrical

measurements as described in chapter 3.5.4 are carried out. Output characteristics of all the sample devices with different line widths and changing line thicknesses of the PEDOT:PSS electrodes are recorded. The values that are compared are the on/off ratio and the on-current. In figure 4.6 the influence of the varying thickness on the on/off ratio and the progression of the on-current are shown.

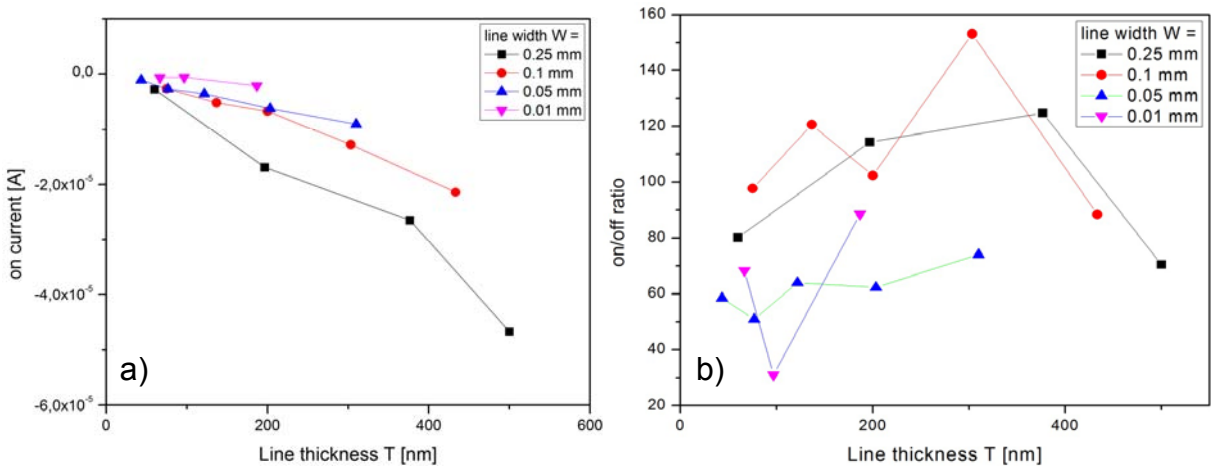

Figure 4.6: a) on-current depending on the line thickness T b) on/off ratio depending on the line thickness T

As seen in figure 4.6 a) the on-current increases with increasing line thickness. This is consistent with the decrease of the sheet resistance with increasing line thickness (figure 4.5). The increase of the conductivity is less visible for lines with a small width. The reason for this is the manufactoring process by inkjet printing. When the line width is small, the diffluence of the first layer of printed ink leads to a percental higher divergence between the predefined and the obtained line width as in broad lines. In our case this discrepancy was 730% for lines with 10 µm predefined line width and 40% for lines with 250 µm predefined line width. For 10 µm lines this strong diffluence leads to a very broad first line. When the following layers are printed on top of this first line, the amount of PEDOT:PSS planned for much smaller lines is distributed all over this line width. This results in a lower percental divergence between the first and the last printed layer for 10 µm lines (6%) than for 250 µm lines (56%) as shown in figure 4.7. Due to this lack of increasing line width, the cross section of the PEDOT:PSS line, determining the on-current, only increases due to the increase of line thickness. In this way the lower increase of the on-current can be explained.

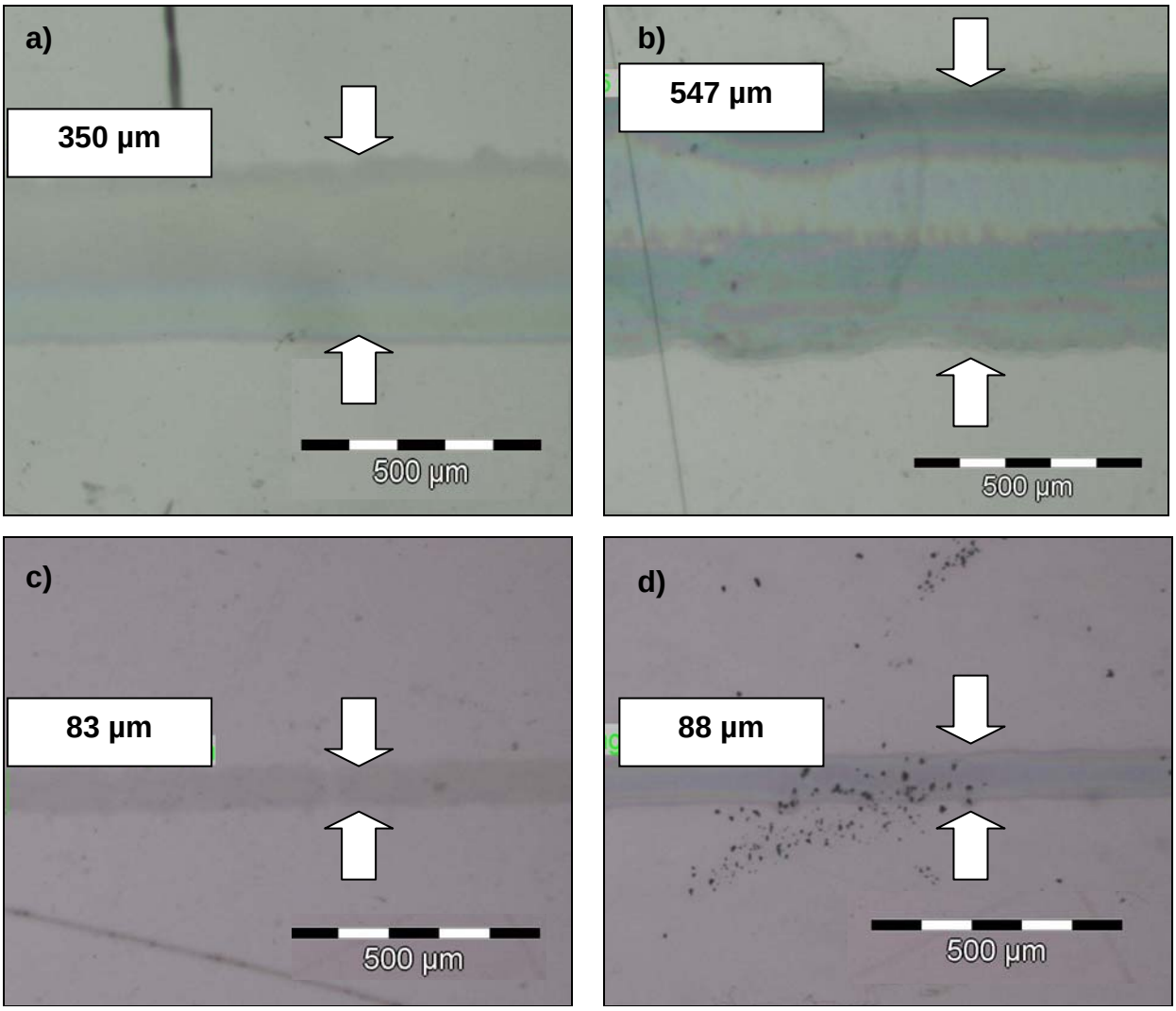

Figure 4.7: a) micrograph of a line with the nominal line width of 250 µm with one layer printed and b) seven layers printed c) micrograph of a line with the nominal line width of 10 µm with one layer printed and b) seven layers printed

Confirmed is this explanation by the depiction of the on-current normalized on the line width shown in figure 4.8 a). With the influence of the line width repealed by dividing the on-current through the real line widths in table 4.1 leaving the on-current only depending on the PEDOT:PSS thickness, all different designs show a on-current in the same range. Additionally, the expected linear dependence of the on-current on the line thickness is visible too. This is depicted by the linear trend line added to the accumulation of the on-currents (figure 4.8 b)) of all different designs showning an coefficient of determination of 0,91.

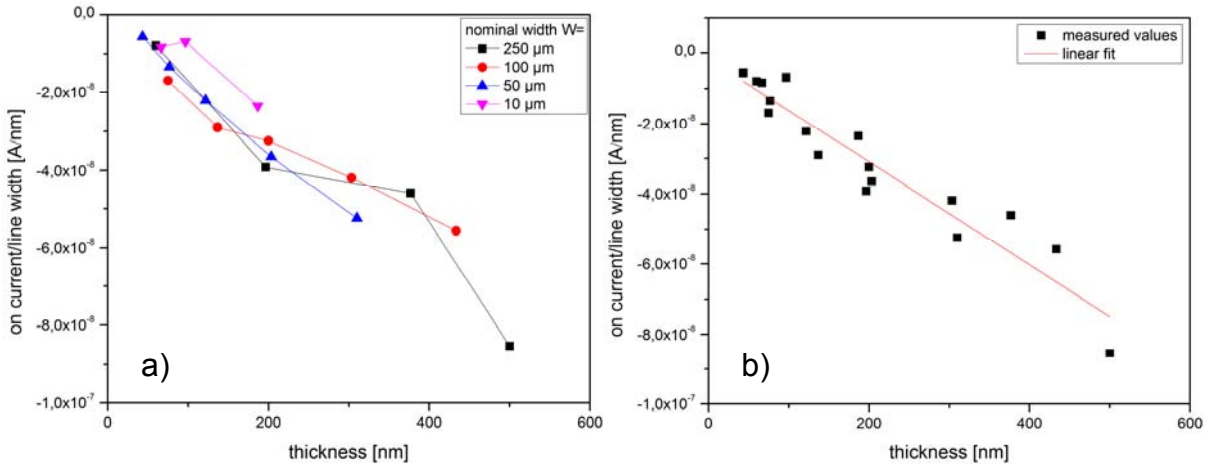

Figure 4.8: a) on-current normalized on the width of the source-drain lines of the different designs b) linear fit of all measured on-currents

Table 4.1 obtained real source-drain line widths with different numbers of PEDOT:PSS layers printed

nominal line width [µm]			10		
layers printed	1	2	3	5	7
real line width [µm]	83	75	83	97	88
nominal line width [µm]			50		
layers printed	1	2	3	5	7
real line width [µm]	189	173	161	170	200
nominal line width [µm]			100		
layers printed	1	2	3	5	7
real line width [µm]	155	177	207	306	384
nominal line width [µm]			250		
layers printed	1	2	3	5	7
real line width [µm]	350	470	432	576	547

The on/off ratio shows some fluctuations but there is no trend in a specific direction noticeable (figure 4.6 b)). An unchanged on/off ratio while the on-current is increasing implies that the off-current is increasing too. This increasing off-current stands for a worse shut down of the transistor. A possible explanation for this effect is the slower reduction of the PEDOT:PSS in the deeper regions of the source-drain line. This leads to a graduation of reduced material during the measurement with mostly unreduced, high conducting material on the bottom of the line, resulting in a higher off-current. The described effect is schematically depicted in figure 4.9 where a cross section through a transistor is shown. The shading blue colour and the white dashed

line represent the reduction front in the source-drain line moving from the top to the bottom of the electrode.

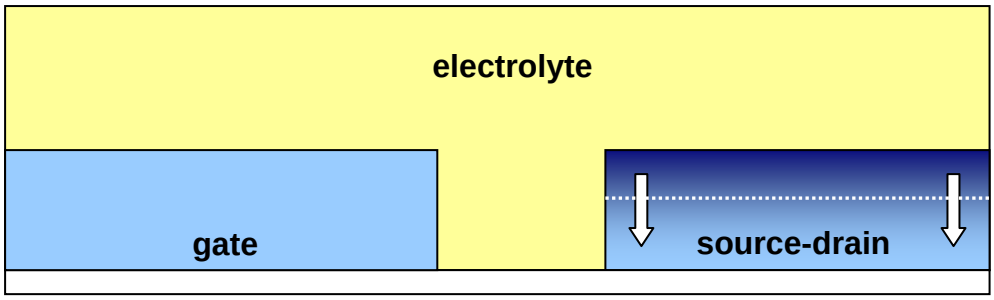

Figure 4.9: scheme of the reduction front, depicted by the shading blue colour and the dashed white line, moving from the top to the bottom of the source-drain line

Variation of the gap between the gate electrode and the source-drain line

Next the gap between the gate and the source-drain line is varied to evaluate its effect on the transistor performance. The designs 2 and 3 shown in figure 4.3 a) are used for these measurements. To obtain the variation of the gap the designs are changed with the help of the pattern design program of the inkjet printer. After printing, the sample devices are characterized electrically with the measuring setup described in chapter 3.5.4. Output characteristics are recorded and the on/off ratios as well as the on-current of the transistors with the varying gaps are compared. The resulting on/off ratio and on-current trends are depicted in figure 4.10.

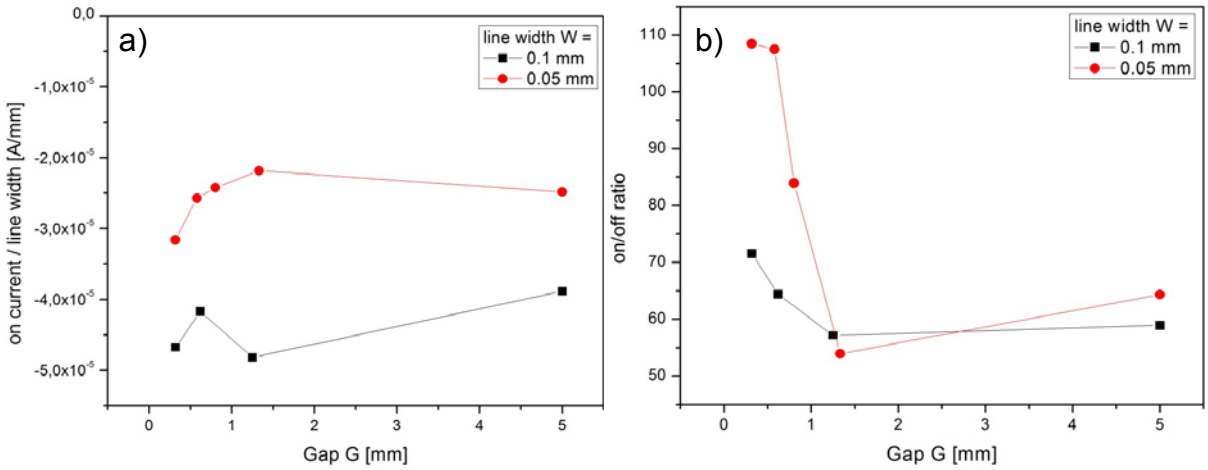

Figure 4.10: a) on-current depending on the gap G b) on/off ratio depending on the gap G

The on-current shows some fluctuation but there is no trend in a specific direction recognizable (figure 4.10 a)). This is expected because the on-current is measured

when there is no gate voltage applied. So there should not be any influence of the gap between the gate and the source-drain line on this value. The on/off ratio clearly increases at small gaps as depicted in figure 4.10 b). An explanation for this may be the measuring speed and the low switching speed of the transistors. When the gap is small enough the measuring time is sufficient to reduce the entire width of the source-drain line and the transistor is shutting down very well. An additional requirement to achive this shut down is a potential, caused by the applied gate voltage that is big enough to move the cations all across the source-drain line and thereby cause a reduction of the whole line width. These two preconditions lead to a low off-current and, in combination with a constant on-current, compared to transistors with bigger gaps to an increasing on/off ratio when the gaps are smaller. When the gap is too big, the reduction of the PEDOT:PSS, that starts at the edge of the source-drain line which is closer to the gate, is too slow to reduce the PEDOT:PSS on the whole line width. This leads to a higher off-current and a worse on/off ratio compared to transistors with smaller gaps. The gradation of the reduction is schematically depicted in figure 4.11, a top view of the transistor, by the blue shading and the dashed white line representing the moving reduction front on the source-drain line. To increase the visibility of the effect the electrolyte is not shown on top of the source-drain line. This effect is enlarged by bigger line widths of the source-drain line because the reduction front has a longer way to move across the line. The larger increase of the on/off ratio at the sample with a line width of 0,05 mm in comparison to the sample with 0,1 mm indicates this second effect. The low on/off ratio of the transistors used for the investigations on the device geometry is comparable to the on/off ratio of the first ECTs described in chapter 4.1.1. A reason for this may be the use of the same substrate. As mentioned before the PET foil used for these transistors was stored at ambient conditions for a long time and its surface showed scratches and other inhomogeneities. These interference factors can have a negative effect on the on/off ratio and explain the obtained low on/off ratios in this way. Despite the fact that the ECTs used to examine the influence of the different device dimensions have low on/off ratios, a trend depicting its influence on the dimensions is very distinctly recognizable.

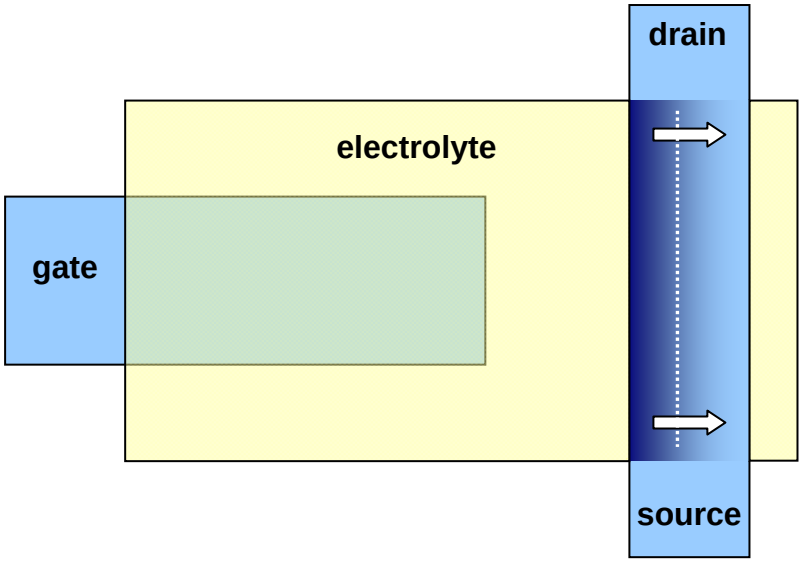

Figure 4.11: reduction front, depicted by the shading blue colour and the dashed white line, moving across the source-drain line in the direction of the arrows

4.2 Entirely inkjet printed ECTs

One goal of this work is the fabrication of ECTs and inverters that are entirely inkjet printed. Those entirely inkjet printed devices have a higher expected uniformity, reproducibility and precision of fabrication. This and the fact that inkjet printing is a manufactoring technique that is not only usable for lab applications but also, due to its high printing rates, suitable for industrial scale production, are reasons to develop entirely inkjet printed ECTs. The PEDOT:PSS for the electrodes is a commercial ink developed especially for inkjet printing. The same is true for the silver ink used for the contact pads. Therefore these inks could be used without any modification. The electrolyte on the other hand is not specified for the inkjet printing process and hence some tuning of the properties has to be carried out.

Adjustment of the viscosity

Despite the low viscosity of Electrolyte 1 it is still too high to make Electrolyte 1 suitable for inkjet printing. The fluid it too viscous to pass through the nozzles of the print head and form drops. To solve this problem the viscosity needs to be lowered to a value suitable for inkjet printing. This is achieved by dilution of the electrolyte with deionized water. Dilutions with volume ratios of one part electrolyte and two parts water (1 + 2) and one part electrolyte and three parts water (1 + 3) are prepared. The electrolyte samples with the lowered viscosity are then printed in test patterns. Squares with increasing sizes are chosen for this printing test (figure 4.12 a)). The smallest square consists of one drop, the next of two times two, the third of three times three and the last of five times five drops of printed electrolyte. With every dilution of the electrolyte four sets of the whole test pattern are printed. The results are shown in figure 4.12 b) to e). The printing direction is from right to left.

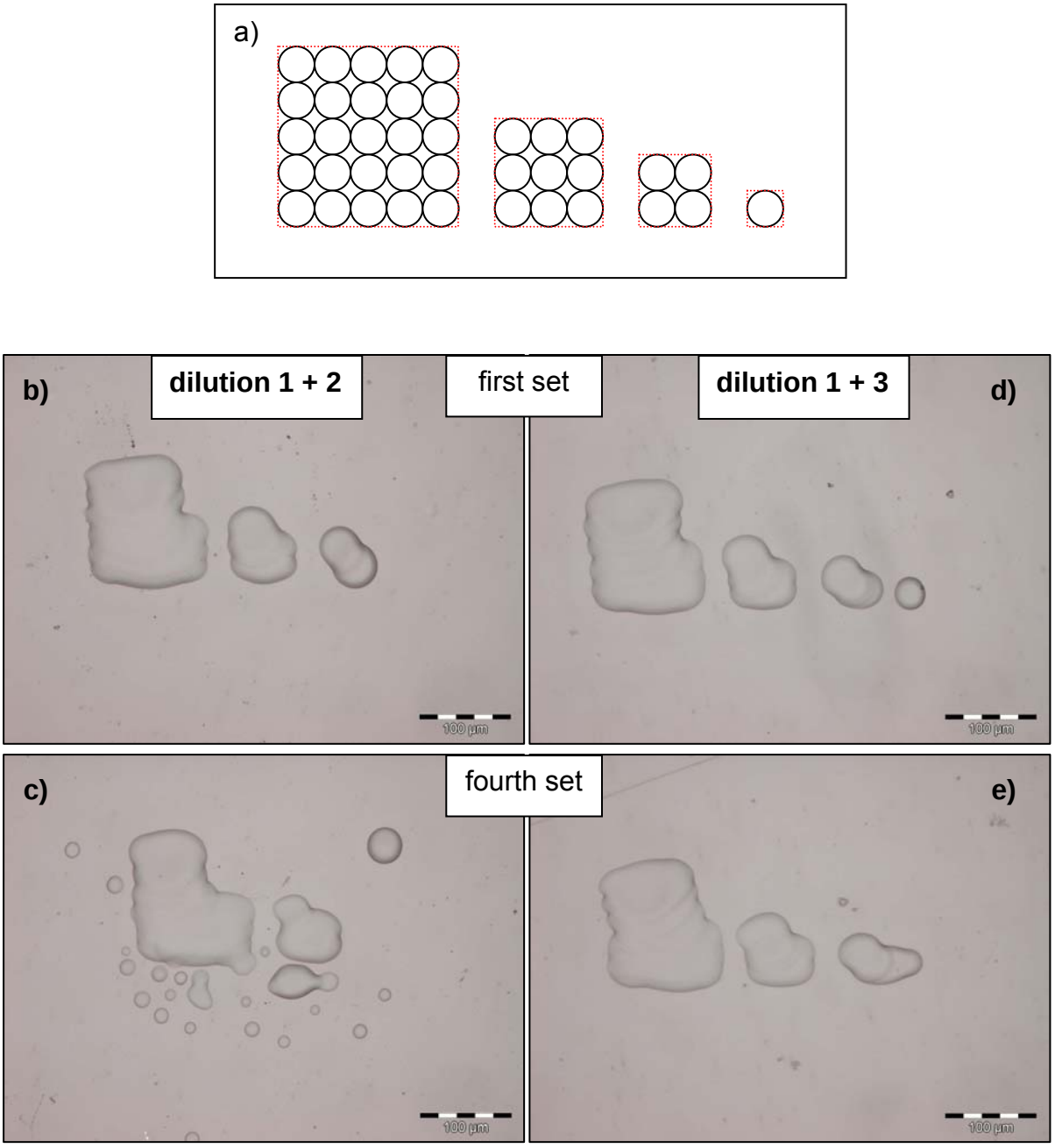

Figure 4.12: a) printing pattern for testing the electrolyte dilutions b) dilution 1 + 2 first printing set c) diltuion 1 + 2 fourth printing set d) dilution 1 + 3 first printing set e) diltuion 1 + 3 fourth printing set

At a dilution of 1 + 2 the smallest square is printed neither in the first (figure 4.12 b)) nor in the fourth set (figure 4.12 c)). Also the shape of the printed pattern is not flawless. At the first set the first drop of every square (notice the print direction from right to left) is missing when the size of the square exceeds the size of the square printed before. A reason for this is that the viscosity is still too high and a second impulse of the piezo crystal in the nozzle is needed to actually release the drop when a new row of drops is started to add up to the pattern. This effect is intensified at the

fourth set where the two smaller squares are not printed at all anymore. Also there is a lot of spraying visible at the picture of the fourth set. The reason for this is the beginning clogging of the nozzles and the high viscous fluid pressed through the partly blocked nozzles. At a dilution of 1 + 3 all four squares are visible at the first set (figure 4.12 d)). Despite the higher dilution and therefore a lower viscosity the effect of the missing first drop in every printed row is still visible, except for the first square that consists only of that first drop. In comparison to the 1 + 2 dillution there is not such a big degradation of the printing quality between the first and the fourth set (figure 4.12 e)) visible. Indeed the first square is connected to the second one and the overall pattern shape is a bit worse but the spraying that occurred at a dilution of 1 + 2 at the fourth set has disappeared for a dilution of 1 + 3. Because the quality of the printing is sufficient and a further lowering of the active material content by further dillution is not desirable, the 1 + 3 dilluted Electrolyte 1 is used for further printing of devices.

Adjustment of the amount of electrolyte

When the electrolyte is applied by hand a very thick, undefined layer is obtained. When it is inkjet printed, the amount and thereby the thickness of electrolyte can be exactly defined. To determine the amount of electrolyte needed to manufacture functional ECTs, different quantities of electrolyte are printed on prepared PEDOT:PSS electrodes. This is achieved by different numbers of layers printed by the inkjet printer. Pictures of those samples are shown in figure 4.13. Afterwards electrical characterisations of the obtained devices are carried out to determine if they show transistor activity or not and in this way identify the minimum amount of electrolyte needed. The resulting output characteristics are shown in figure 4.13.

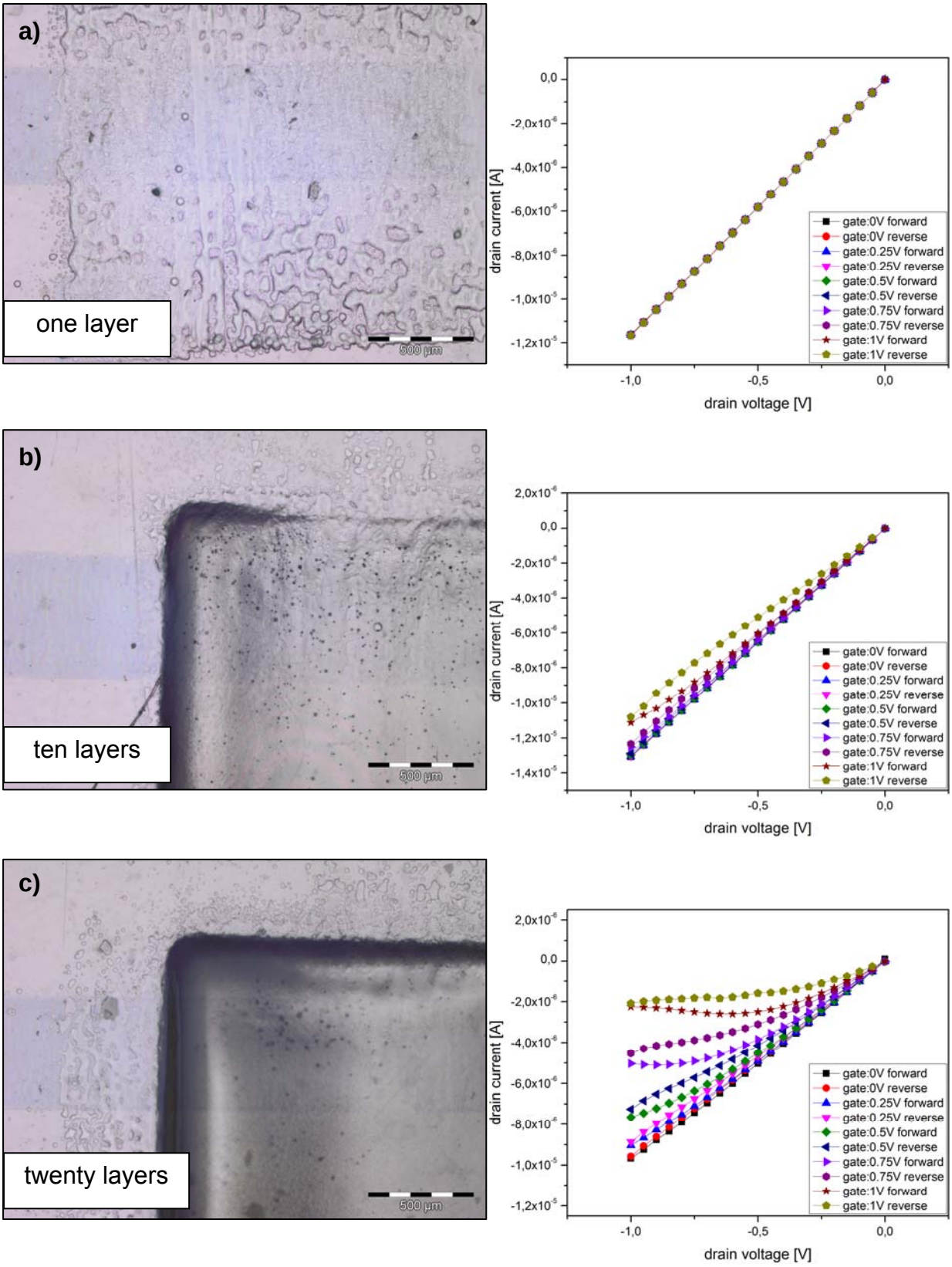

Figure 4.13: photograph and output characteristic of an ECT with a) one layer b) ten layers and c) 20 layers of electrolyte printed

As depicted there is a need for ten layers of electrolyte to show beginning transistor activity and at least twenty layers to show sufficient transistor activity. There are two

different possible explanations for the fact that there is a need for several layers of electrolyte to build a working device. The first is the amount of active material contained in the electrolyte. If the quantity of electrolyte and thereby the amount of available active material is too low no reduction of the PEDOT:PSS can occur and the sample does not show transistor behaviour. The second possible reason is the drying behaviour of the electrolyte. It is assumed that at ambient conditions thicker layers of electrolyte dry at the edges and encapsulate liquid electrolyte inside. If the layer is too thin and the electrolyte is drying out completely through the whole layer, the mobility of the cations is limited and thereby no or only limited transistor behaviour is shown. This functionality limiting effect is confirmed by the fact that a previously working transistor (figure 4.14 a)) left in the glovebox, that can be assumed to be dried out, does not show sufficient functionality any more (figure 4.14 b)). To confirm that this lack of functionality is a result of the missing moisture, the sample is electrically characterised again after leaving it at ambient conditions for 24 hours and allowing the electrolyte to absorb humidity again. After this, transistor behaviour is shown again (figure 4.14 c)). Also examinations on a working sample dried on a hot plate confirm this drying-out effect on the functionality of the devices. A previously funtional transistor (figure 4.14 d)) is dried on a hot plate at 60°C for 120 minutes and characterised electrically afterwards. No transistor activity is visible as shown in figure 4.14 e). After treating the sample with a spray of fine water droplets and thus increasing the moisture of the electrolyte, transistor behaviour is visible again (figure 4.14 f)). These two experiments confirm the direct relation between the moisture of the electrolyte and the functionality of the transistor and approve the need for a thicker layer of electrolyte to manufacture functional, entirely inkjet printed electrochemical transistors.

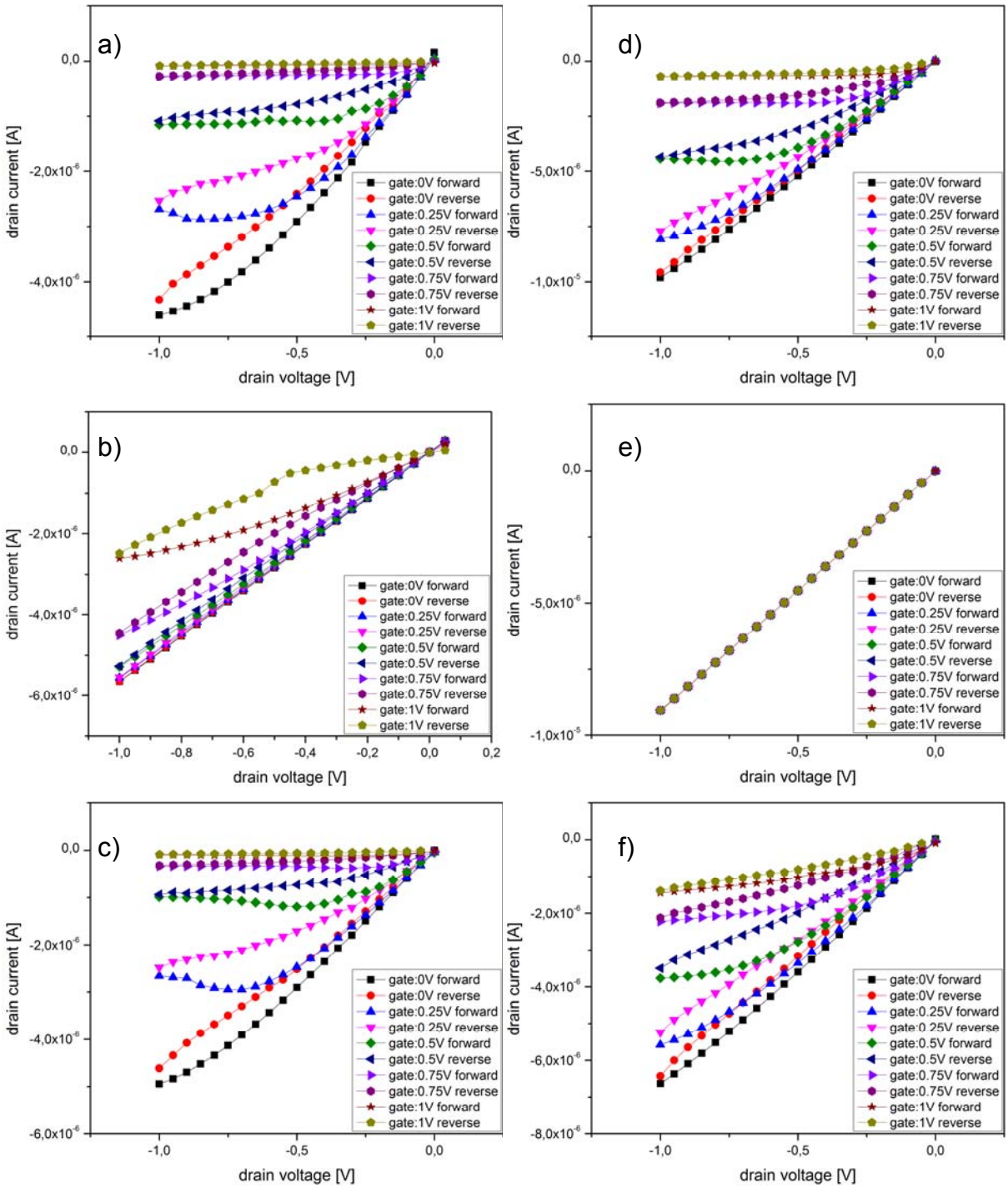

Figure 4.14: output characteristics of an ECT a) before drying b) in a glovebox c) after 24 hours at ambient conditions to re-absorb humidity; output characteristics of an ECT d) before drying e) directly after drying on a hot plate for 120 minutes at 60°C f) after treatment with fine water droplets

4.2.1 ECTs on a modified substrate

In electronics it is common to build devices as small as possible to increase their number on a certain area. To achieve a size reduction of the ECTs the width of the source-drain line needs to be small because the size of the gate depends on the

width of this line. Small lines lead to possible small gates and to small devices. With our inkjet printer the minimum achievable line width of PEDOT:PSS on PET foil is 60 µm. A decrease of this value demands the change of the substrates surface properties. Because the Clevios P Jet HC ink is waterbased, smaller line widths can be obtained when the surface wettability is decreased. To achieve this, a UV curable photoresist, microresist® UVcur06 [52], is spun on the surface of the PET foil and cured under UV light in vacuum. The hydrophobicity of this resist is high enough to obtain small lines but still low enough so that lines, and not only unconnected drops of ink, are formed. With the substrate modified in this way PEDOT:PSS line widths below 10 µm are achieved. Silver contact pads and an electrolyte spot are printed in a matching size completing an entirely inkjet printed ECTs (figure 4.15 a)). The line width of the PEDOT:PSS electrodes is 6 µm (figure 4.15 a) inset) which is smaller than the minimum predefinable line width of 10 µm in the printing pattern. This smallest predefinable value can be considered as the resolution limit of the used inkjet printer. The obtained transistors are electrically characterized afterwards. An output characteristic is shown in figure 4.15 b).

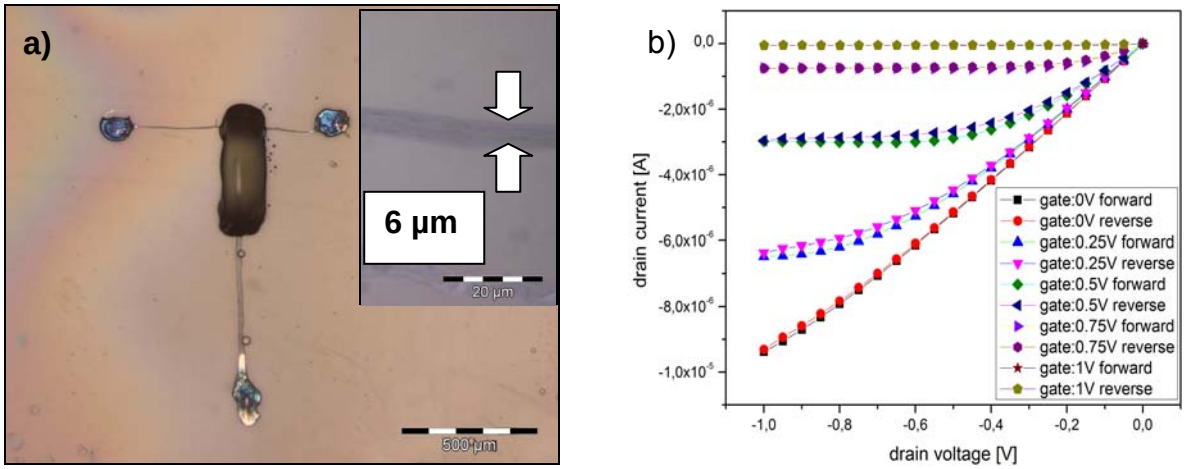

Figure 4.15: a) micrograph of an ECT on a modified substrate with a source-drain line width of 6 µm, a gap between the gate electrode and the source-drain line of 100 µm and an area ratio between the gate electrode and the active area on the source-drain line of 6:1 Inset: line width of source-drain line b) output characteristic of an ECT on modified substrate

As depicted in figure 4.15 b) the ECTs printed on modified substrate show transistor behaviour. Clearly recognizable is the lower hystereses of only h_{max} = 1,4·10^{-7} A at a gate voltage of V_g = 0 V. The on-current of I_{on} = -9,1·10^{-6} A is comparable to ECTs where the same amount of PEDOT:PSS is printed on the unmodified substrate. The

off-current on the other hand with I_{off} = -4,7·10^{-8} A is higher, leading to a lower on/off ratio of 140. A reason for this could be the larger line thickness of 450 nm and thereby a smaller surface to volume ratio. Considering that the reduction starts at the interface of the PEDOT:PSS electrode and the electrolyte and afterwards continues in the bulk electrode this may lead to a worse shut down of the device during the limited measuring time. Additionally the ratio between the gate area and the active area of the source-drain line is less then the ratio of 10:1 suggested in the literature [31]. The problem regarding the area ratio could be remedied by adjusting the printing pattern and hence the design of the ECT. The goal to show the possibility to fabricate electrochemical transistors with line widths below 10 µm by changing the substrate is reached with the devices shown in this chapter. So as next step transistors suitable for building inverters are fabricated.

4.2.2 ECTs for inverters

To fabricate a logic gate, the inverter, entirely inkjet printed transistors on PET foil are used. These transistors have a source-drain line width of 250 µm and a ratio between the gate area and the active area of the source-drain line of 12:1. The reproducibility of those devices is very high. A micrograph of an ECT used to build an inverter as well as an output characteristic is shown in figure 4.16.

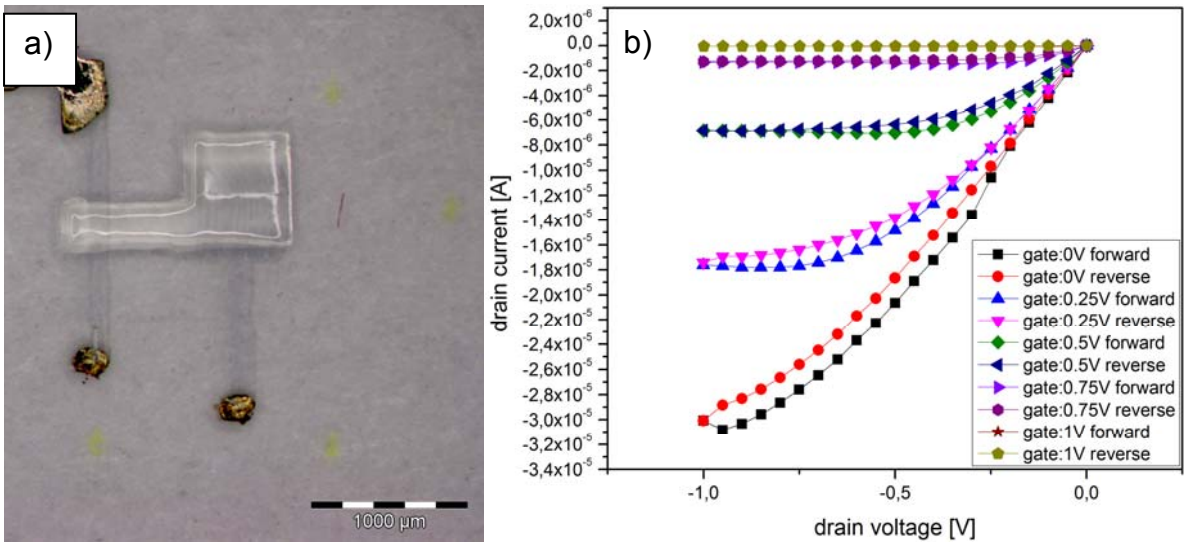

Figure 4.16: a) micrograph and b) output characteristic of an ECT used for inverters with a source-drain line width of 250 µm, a gap between the gate electrode and the source-drain line of 500 µm and an area ratio between the gate electrode and the active area on the source-drain line of 12:1

The output characteristics show a decent saturation of the drain current and a maximum hystereses of h_{max} = $1 \cdot 10^{-6}$ A at a gate voltage of V_g = 0 V. Due to the broader lines and therefore a larger cross section area the on-current of I_{on} = $-3 \cdot 10^{-5}$ A is higher than the on-current of the previously described transistors. With the off-current of I_{off} = $-5{,}2 \cdot 10^{-8}$ A in the same range a higher on/off ratio of 575 is obtained. The reason for this is an appropriate area ratio of the gate area to the active area on the soucre-drain line. Additionally the surface to volume ratio of the source-drain line is higher leading to a bigger interface of electrolyte and PEDOT:PSS. In this way a sufficient on/off ratio is obtained. The on-current as well as the off-current are included in the calculations to design the inverters based on ECTs (see chapter 2.4). More important than the value is the reproducibility of these currents. As long as it is reproducible the design of the inverter can be adjusted to fit the currents. But for both, the on-current and the off-current, there exist minimum requirements (see chapter 2.4). The obtained transistors performance with an on-current of I_{on} = $-3 \cdot 10^{-5}$ A and an off-current of I_{off} = $-5{,}2 \cdot 10^{-8}$ A is within the range for building functional inverters.

4.3 All inkjet printed inverters based on ECTs

The transistors described in the last chapter enable us to fabricate inkjet printed inverters. These inverters are the first step from electrochemical transistors towards logic circuits because it is possible to drive one inverter with the output signal of a preceding inverter. In chapter 2.4 the requirements for these inverters are described. The voltage divider that is needed to change the negative output voltage of the ECT into a positive voltage also consists of inkjet printed PEDOT:PSS resistors. A micrograph of such an inverter, which is entirely fabricated by inkjet printing, is shown in figure 4.17 a). The inverters are electrically characterized with the setup in chapter 3.5.4. The transfer characteristic and the gain of these inverters are shown in figure 4.17 b) and c).

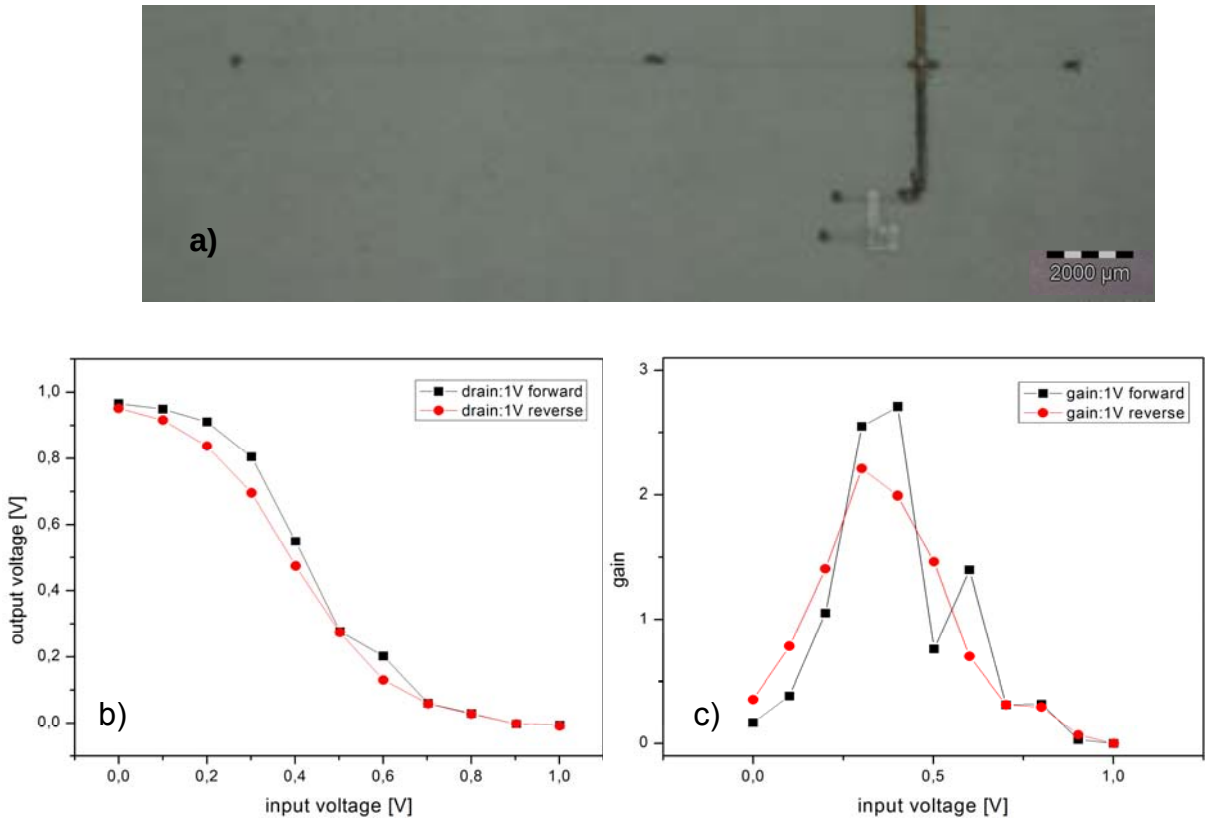

Figure 4.17: a) micrograph b) transfer characteristic and c) gain of an entirely inkjet printed inverter

The transfer characteristics of the inverter show plateaus at the high and the low level. The voltage of the high level where the transistor is switched on is V_{out} = 0,97 V and the voltage of the low level where the transistor is switched off is V_{out} = –0,01 V. Requested is a voltage for the high level of 1 V and for the low level of 0 V. The supply voltages of +3 V and –3 V are suggested by Nilsson et al. [41]. Considering the

resistance of the switched on respectively off transistor of R_{ON} = 32 kΩ and R_{OFF} = 18MΩ following resistors are fabricated by inkjet printing: R1 : R2 : R3 = 427 kΩ : 280 kΩ : 154 kΩ = 7,93 : 5,20 : 2,86. For the idealized cases described in chapter 2.4 equations 2.3 to 2.6 output voltages of V_{out} = 1,26 V for the on state and V_{out} = 0,02 V for the off state of the transistor are calculated. The output voltage for the on state of the transistor differs significantly from the measured value for V_{out}, suggesting that the idealized calculation method is unrewarding and the more realistic of the "Helmoltz´sche Überlagerungssatz" has to be performed. With this calculation method, described in chapter 2.4 equations 2.7ff, output voltages of V_{out} = 0,95 V for the on state and V_{out} = 0,03 V for the off state of the transistor are calculated. These calculated values, with the on state value much closer to the measured values, suggest that this calculation method is more adequate to represent the real inverters. Also these calculations confirm that the ratio of the resistors as well as the supply voltages are appropriate, approving the measured output voltage values. Generally, these transfer characteristics and calculations confirm the derived design of the inverters. Moreover the gain of the inverter is proper for an inverter based on a electrochemical transistor [41]. The gain of 2,7 may seem low compared to a complementary organic inverter where a gain in the range of 10^2 is common [61], but the design and concept of inverters based on electrochemical transistors are completely different, so a direct comparison on a quantitative basis is not appropriate (see chapter 2.4). In summary, the performance of the inverters based on electrochemical transistors is satisfying and the chosen design can be considered as functional. The next step is the dynamic characterisation of the inverters to determine their behaviour when a series of consecutive on and off input signals are applied. This is necessary in order to verify the usability for logic circuits and to determine the switching speed. The used measuring setup is described in chapter 3.5.4. A typical response of the device for a square wave input signal with a frequency of 0,05 Hz is shown in figure 4.18 a). These response characteristics are recorded with an oszilloscope. Also a single spike is depicted for a graphic extraction of the switching speed of the inverter (figure 4.18 b)).

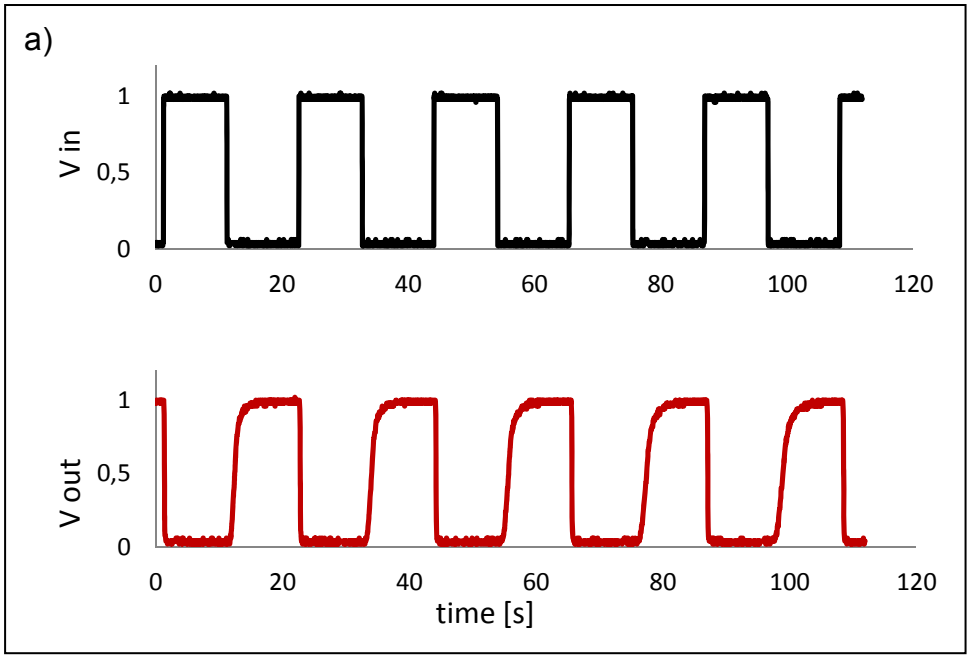

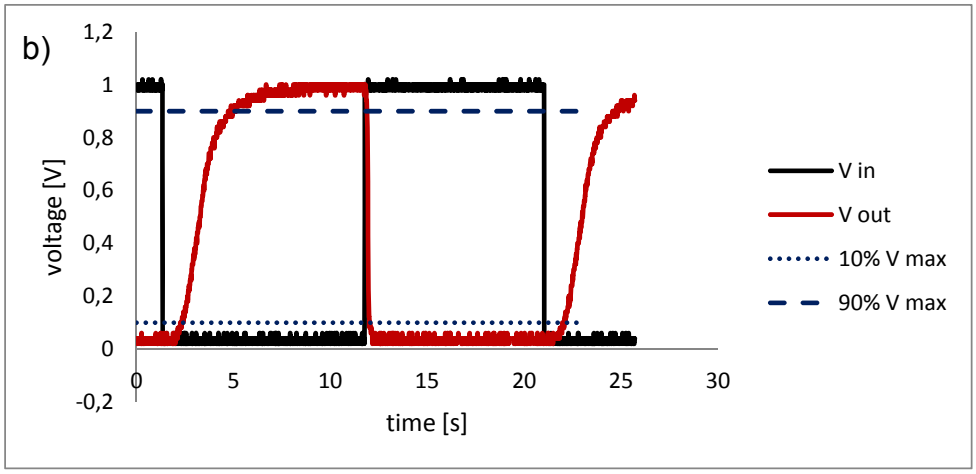

Figure 4.18: a) response characteristics for an electrochemical inverter b) single spike for graphical determination of the switching speed

Figure 4.18 a) shows high and low levels of +1 V and 0 V respectively that are constant for a measuring period of 110 seconds. Also a fast response of the output voltage on the square wave input signal, depicted by a very small shift of the two signals, is visible. Additionally, a difference in the speed of switching the transistor on and back off again can be seen in this figure. This difference is even more obvious in the enlargement of one spike shown in figure 4.18 b). It takes 3,3 seconds to get from 0V to 90% of the maximum voltage of 1 V and 0,4 seconds to get from 1 V back to 10% of the maximum. These switching times are graphically determined. An explanation for this mismatch of switching speeds may be the edge of the reduction front. During the reduction process it is possible that this front is moving beyond the

electrolyte edge towards the drain electrode (figure 4.19). In this case the reverse process of oxidizing the PEDOT and returning to the conducting state of PEDOT:PSS takes more time because the electrolyte triggering the reaction is not in direct contact with the PEDOT [41]. A direct comparison of the switching speed of our inverters to the dynamic behaviour of inverters described in literature is not possible due to a different measuring method [41]. Based on a characterisation by building ring oscillators and measuring their response characteristics, switching speeds of 10 seconds for one device are achived. Our devices where measured as single devices with a square wave input signal of 0,05 Hz leading to a switching cycle of 20 seconds, but this is not the maximum achievable speed. The response characteristics in figure 4.18 a), showing pronounced plateaus between the on- and off-switching phase, suggest that a switching speed in the range of 10 seconds of our all inkjet printed inverters, which is in the range of the inverters shown in literature, is possible.

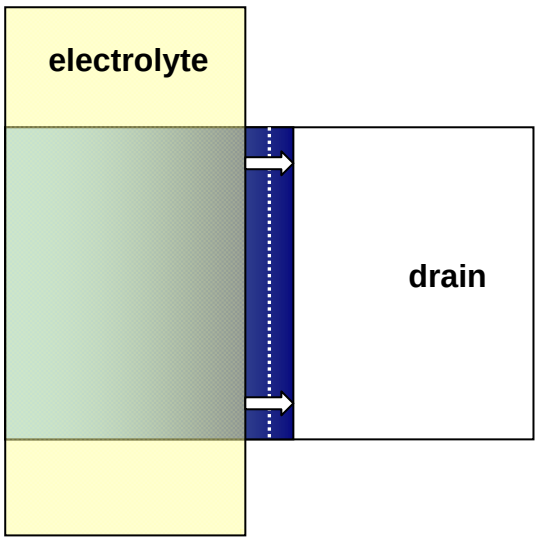

Figure 4.19: scheme of the reduction front, depicted by the shading blue color and the dashed white line, moving beyond the edge of the electrolyte

5 Summary and Outlook

The first task of this work was the fabrication of electrochemical transistors with inkjet printed PEDOT:PSS electrodes and a polyelectrolyte applied by hand. With this setting the possibility to fabricate functional transistors using inkjet printed PEDOT:PSS in combination with a polyelectrolyte is examined. The resulting devices show transistor behaviour and an on-current that is suitable for organic electronics, but a low on/off ratio. Although the performance of this first ECTs is not entirely satisfying, the functionality of these devices, combining inkjet printed PEDOT:PSS as electrodes and a polyelectrolyte, is confirmed.

As a next step two different electrolytes are compared. These electrolytes differ in their used anions, cations and their overall formulation. To determine the influence of the electrolyte on the transistor behaviour, devices with the same geometry are used for these evaluations. The electrical characterisations show hardly any difference. The on-current, the on/off ratio and also the hystereses are nearly similar. In their physical properites the electrolytes show a very prominent difference, their viscosity. One electrolyte is well suited for inkjet printing while the other one can be processed by screen printing. Summerizing, two electrolytes with nearly similar performance but differing processing possibilities are available with the two examined electrolytes.

A very important result is the examined influence of changing ECT geometries on the transistor performance. The parameters of the transistor geometry that were varied are: (i) The thickness of the PEDOT:PSS lines controlled by the number of printed layers of PEDOT : PSS and (ii) the gap between the gate and the source to drain line. (iii) These variations were made for transistors with different line widths. The area ratio between the gate electrode area and the active area on the source-drain line remains unchanged due to its influence on the transistor performance that should be excluded from these evaluations. The devices with the changing geometry are electrically characterized and the resulting on-currents and on/off ratios are compared. The results, examining devices with different line widths and varying line thicknesses, are: (i) The on/off ratio is not influenced by an increasing thickness of

the PEDOT:PSS electrodes and (ii) the on-current is increasing with an increasing PEDOT:PSS thickness. Due to the diffluence of the PEDOT:PSS ink during the printing process the on-current increases less at small lines than at broad lines. With this influence repealed by considering the obtained real line widths all transistors with different nominal line widths show on-currents in the same range. On closer examination these results reveal that an increasing on-current with a constant on/off ratio imply an increasing off-current, standing for a worse shut-down of the transistor. For building ECTs this means that an increasing line thickness results in a higher on-current and, due to an increasing off-current, a constant on/off ratio.

When the gap between the source-drain line and the gate electrode is varied the results are: (i) The on-current remains basically unchanged and (ii) the on/off ratio is increasing with a decreasing gap between the gate electrode and the source-drain line (figure 5.1). Considering the constant on-current and the increasing on/off ratio, the off-current has to decrease when the varied gap is increasing, standing for a better shut-down of the transistor.

For fabricating transistors it has to be taken into account that increasing gaps between the gate electrode and the source-drain line lead to an unchanged on-current and an increasing on/off ratio. Because the on/off ratio is an important parameter for ECTs, especially when the use in logic circuits is planned, these results are very helpful.

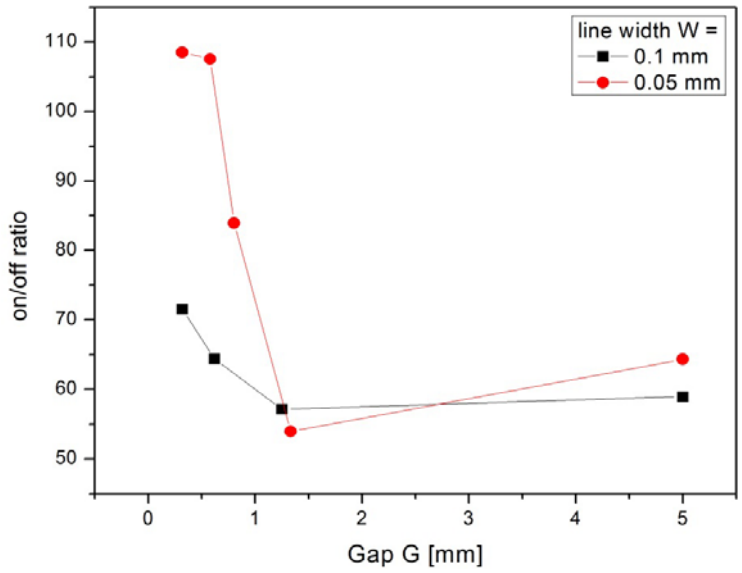

Figure 5.1: on/off ratio depending on the gap between gate electrode and source-drain line

One goal of this work is the fabrication of ECTs that are entirely inkjet printed. Investigations on the inkjet printing behaviour of the electrolyte have to be carried out to make this possible.
Firstly the viscosity of the electrolyte has to be lowered by dilution with deionized water to obtain a viscosity that allows for reasonable printing results. Second the amount of electrolyte needed to achieve sufficient transistor activity is evaluated by electrical characterisations of transistors with different amounts of electrolyte applied. Results show that an electrolyte layer with a thickness of 50 µm is necessary to provide enough mobile charge carriers and thus achieve sufficient transistor activity.
With the modified electrolyte and the commercial PEDOT:PSS ink especially developed for inkjet printing it is possible to fabricate entirely inkjet printed electrochemical transistors.
Using a substrate with a modified surface wettability, transistors with a source-drain line width of 6 µm are fabricated. Line widths in that range can be assumed to be the resolution limit of the used inkjet printer. The ECTs show satisfying transistor behaviour with noticeable low hystereses and approve the possibility to obtain very small inkjet printed lines by changing the substrates surface properties.

Based on ECTs additionally all inkjet printed inverters are fabricated. The design of the inverters is derived from literature data, calculations concerning the used transistors and practical evaluations. The resulting inverters are operated by a positive voltage input signal and provide a positive voltage output signal. This ensures that one inverter can control a subsequent inverter.
With their functionality confirmed, the electrochemical inverters are dynamically characterized. This is necessary in order to verify the usability for logic circuits and to determine the switching speed. The response of an inverter on a square wave input signal is examined by recording the input signal and the resulting output signal using an oszilloscope (figure 5.2). The fast response of the inverter on the input signal is visible, although the switching speed limit is not reached. The plateaus between the on- and off-switching suggest that also a higher frequency input signal could be processed by these electrochemical inverters.

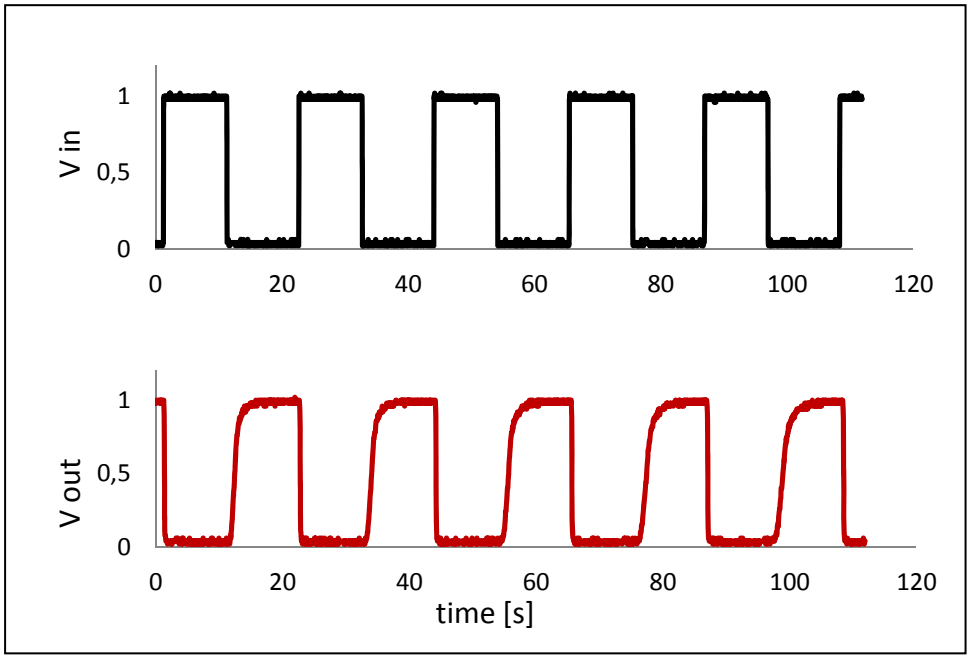

Figure 5.2: response characteristic of an electrochemical inverter

Further research effort should be put into the transistors printed on a modified substrate. The very small hystereses, making them well suited for the use in logic circuits, is a big advantage. So further effort should be put into examinations of the design and possible enhancement of the fabrication process of those transitors.

To lower the influence of the environment, especially the humidity, on the properties of the electrolyte and thus on the performance of the transistors, the possibilities for a proper encapsulation of the electrolyte need to be evaluated. In this way the uniformity of the devices could be further enhanced.

Further research on the dynamic behaviour of the inverters based on electrochemical transistors should be carried out. Especially the influence of changing transistors dimensions on the dynamic performance of the inverters should be examined. Also the possibilities to lower the asymetric switching behaviour by changing the design should be the aim of further research.

Because it is assumed that the overall dimensions of the device have an influence on the switching speed, smaller devices should be examined. An additional advantage of smaller devices would be the higher density of devices on a certain area.

To achieve this a different way of structuring the PEDOT:PSS electrodes needs to be applied because the limit for reproducible electrodes fabricated by inkjet printing seems to be reached with the transistors described in this work. Possible manufactoring ways may be photolithography or nanoimprint lithography processes.

When the dimensions are reduced also a possible influence on the inverters properties needs to be examined.

Bibliography

[1] Shirakawa, H., Louise, E. J., MacDiarmid, A.G., Chiang, C. K., and Heeger, A. J. (1977). *Journal of the Chemical Society, Chemical Communications*, 578-580

[2] Brütting, W., Frischeisen, J., Scholz, B. J., & Schmidt, T. D. (2011). *Europhysics News*, *42*(4), 20-24.

[3] Malti, A., Gabrielsson, E.O., Berggren, M., & Crispin, X. (2011). *Applied Physics Letters*, *99*(6)

[4] Po, R., Carbonera, C., Bernardi, A., Tinti, F., & Camaioni, N. (2012). *Solar Energy Materials and Solar Cells*, *100*, 97-114.

[5] Alvarez, A., Costa-Fernández, J. M., Pereiro, R., Sanz-Medel, A., & Salinas-Castillo, A. (2011). *TrAC Trends in Analytical Chemistry*, *30*(9), 1513-1525.

[6] a) Andersson, P., Forchheimer, R., Tehrani, P., & Berggren, M. (2007). *Advanced Functional Materials*, *17*(16), 3074-3082. b) Someya, T., Kato, Y., Sekitani, T., Iba, S., Noguchi, Y., Murase, Y., Kawaguchi, H., et al. (2005). *Proceedings of the National Academy of Sciences of the United States of America*, *102*(35), 12321-5.

[7] Andersson, P., Nilsson, D., Svensson, P.-O., Chen, M., Malmström, A., Remonen, T., Kugler, T., et al. (2002). *Advanced Materials*, *14*(20), 1460-1464.

[8] Zirkl, M., Sawatdee, A., Helbig, U., Krause, M., Scheipl, G., Kraker, E., Ersman, P. A., et al. (2011). *Advanced Materials*, *23*, 2069-2074.

[9] Kawase, T., Sirringhaus, H., Friend, R. H., & Shimoda, T. (2001). *Advanced Materials*, *13*(21), 1601-1605.

[10] a) Bailo, D., Generosi, a., Albertini, V. R., Caminiti, R., De Bettignies, R., & Paci, B. (2012). *Synthetic Metals*, *162*(9-10), 808-812. b) Liu, X., Yan, J., Meng, L., Sun, C., Hu, X., Chen, P., Zhou, S., et al. (2012). *Thin Solid Films*, *520*(7), 2979-2983.

[11] Elschner, A., Kirchmeyer, S., Lövenich, W., Merker, U., Reuter, K.: *PEDOT, Principles and Applications of an Intrinsically Conductive Polymer* . CRC Press, Taylor and Francis Group, 6000 Broken Sound Parkway NW, Suite 300 Boca Raton, FL 33487-2742, 2011, ISBN 978-1-4200-6911-2.

[12] Jonas, F., Schrader, L. (1991) *Synthetic Metals, 41–43*, p. 831

[13] Yamamoto, T., Abla, M. (1999) *Synthetic Metals* 100 (2), Pages 237–239

[14] Meng, H., Perepichka, D. F. and Wudl, F. (2003), Angewandte Chemie Internationale Edition 42 (6)

[15] Shiraishi, K., Kanbara, T., Yamamoto, T., & Groenendaal, L. (2001). *Polymer*, *42*, 7229-7232.

[16] Groenendaal, L., Zotti, G., Aubert, P.-H., Waybright, S. M., & Reynolds, J. R. (2003). *Advanced Materials*, *15*(11), 855-879.

[17] Bayer AG, Eur. Patent 440 957, 1991

[18] Groenendaal, B. L., Jonas, F., Freitag, D., Pielartzik, H., & Reynolds, J. R. (2000). *Advanced Materials*, *12*(7), 481-494.

[19] Salaneck, W.R., Friend, R.H., Bredas, J.L. (1999) *Physics Reports 319* p. 231-251

[20] http://www.citycollegiate.com/organic9.htm, June 2012

[21] Johansson, T., Mammo, W., Svensson, M., Andersson, M. R., & Inganäs, O. (2003). *Journal of Materials Chemistry*, *13*(6), 1316.

[22] Dkhissi, A., Louwet, F., Groenendaal, L., Beljonne, D., Lazzaroni, R., & Br, J. L. (2002). *Chemical Physics Letters*, *359*, 466-472.

[23] Kim, J. Y., Jung, J. H., Lee, D. E., & Joo, J. (2002). *Synthetic Metals*, *126*, 311-316.

[24] Miyamoto, T., and Shibayama, K. (1973) *Journal of Applied Physics 44*, 5372

[25] Johansson, T., Pettersson, L. A. A., & Ingana, O. (2002). *Metals, 129*, 269-274.

[26] Zykwinska, a., Domagala, W., & Lapkowski, M. (2003). *Electrochemistry Communications*, *5*(7), 603-608.

[27] Herlogsson, L. (2011). *Electrolyte-Gated Organic Thin-Film Transistors*, Linköping Studies in Science and Technology, Dissertations, No. 1389

[28] Carl H. Hamann, Wolf Vielstich: *Elektrochemie I: Elektrolytische Leitfähigkeit, Potentiale, Phasengrenzen*. 2. Auflage. VCH Verlagsgesellschaft mbH, Oldenburg und Bonn 1985, ISBN 3-527-21100-4.

[29] Kergoat, L., Herlogsson, L., Braga, D., Piro, B., Pham, M.-C., Crispin, X., Berggren, M., et al. (2010). *Advanced materials (Deerfield Beach, Fla.)*, *22*(23), 2565-9.

[30] Basiricò, L., Cosseddu, P., Fraboni, B., & Bonfiglio, A. (2011). *Thin Solid Films*, *520*(4), 1291-1294. Elsevier B.V. doi:10.1016/j.tsf.2011.04.188

[31] Nilsson, D. (2005). *An Organic Electrochemical Transistor for Printed Sensors and Logic*. *Advanced Materials*. Linköping Studies in Science and Technology, Dissertations, No. 921

[32] Panzer, M. J., Frisbie, C. D. (2007). *Journal of the American Chemical Society*, *129*(20), 7824-30.

[33] MacFarlane, D. R., Forsyth, M., Howlett, P. C., Pringle, J. M., Sun, J., Annat, G., Neil, W., et al. (2007). *Accounts of chemical research*, *40*(11), 1165-73.

[34] Lee, J., Panzer, M. J., He, Y., Lodge, T. P., & Frisbie, C. D. (2007). *Journal of the American Chemical Society*, *129*(15), 4532-3.

[35] MacDiarmid, A.G. (2001). *Current Applied Physics*, *1*(4-5), 269-279.

[36] Nilsson, B. D., Chen, M., Kugler, T., Remonen, T., Armgarth, M., & Berggren, M. (2002). *Advanced Materials*, *14*(1), 51-54.

[37] Larsson, O. (2004). *Empirical parameterization of organic electrochemical transistors,* Linköping Department of Science and Technology, Examensarbete

[38] Ujvári, M., Takács, M., Vesztergom, S., Bazsó, F., Ujhelyi, F., & Láng, G. G. (2011). *Journal of Solid State Electrochemistry*, *15*(11-12), 2341-2349.

[39] Zykwinska, a., Domagala, W., Pilawa, B., & Lapkowski, M. (2005). *Electrochimica Acta*, *50*(7-8), 1625-1633.

[40] Rothländer, T. (2010) *Organic Electronics: Complementary Inverters and Ring Oscillators*, Graz University of Technology, Diplomarbeit

[41] Nilsson, D., Robinson, N., Berggren, M., & Forchheimer, R. (2005). *Advanced Materials*, *17*(3), 353-358.

[42] Isaksson, J., Tengstedt, C., Fahlman, M., Robinson, N., & Berggren, M. (2004). *Advanced Materials*, *16*(4), 316-320.

[43] Dimatix® DMP-2800 Product Description, http://www.fujifilmusa.com/products/industrial_inkjet_printheads/deposition-products/dmp-2800/index.html, June 2012

[44] Dimatix® Materials Printer DMP-2800 User Manual Rev.12, Ver.1.5

[45] Dimatix® Industrial Inkjet Cartridge Product Description. http://www.fujifilmusa.com/products/industrial_inkjet_printheads/deposition-products/materials-cartridge/index.html, June 2012

[46] Dimatix® Materials Printer Jettable Fluid Formulation Guidelines, http://www.fujifilmusa.com/shared/bin/Dimatix-Materials-Printer-Jettable-Fluid-Formulation-Guidelines.pdf, June 2012

[47] Laurell® Technologies Spin Coater Literature, http://www.laurell.com/info/literature.php, June 2012

[48] DuPont® Melinex 504 Datasheet, http://www.dupontteijinfilms.com/filmenterprise/Datasheet.asp?Result=Print&ID=269&Version=US, June 2012

[49] CLEVIOS™ P JET HC Datasheet, http://clevios.com/media/webmedia_local/media/datenblaetter/81077108_CLEVIOS_P_JET_HC_20110411.pdf, June 2012

[50] Electrolube® Product Description, http://www.electrolube.com/055/products/tds/SCP.pdf, June 2012

[51] DuPont® Melinex 725Datasheet: http://www.dupontteijinfilms.com/filmenterprise/Datasheet.asp?Result=Print&ID=194&Version=US, June 2012

[52] Vogler, M., Wiedenberg, S., Muhlberger, M., Bergmair, I., Glinsner, T., Schmidt, H., Kley, E., et al. (2007). *Microelectronic Engineering*, *84*(5-8), 984-988.

[53] Cabot® Conductive Ink CCI 300 Datasheet and MSDS, http://www.cabot-corp.com/wcm/download/en-us/nb/ATTH4YZ5.doc, http://www.cabot-corp.com/wcm/msds/en-gb/NB/CCI-300-EUR-EN.pdf, June 2012

[54] http://en.wikipedia.org/wiki/File:Microscope-optical_path.svg, June 2012

[55] Geometric Factors in Four Point Resistivity Measurements, http://www.fourpointprobes.com/haldor.html, June 2012

[56] Veeco® Dektak 150 Surface Profiler, User Manual 2007 Revision A

[57] Haas, U. (2006) Organic Thin Film Transistors with Critical Dimensions in the Nanometer Scale- Nanoimprint Lithography as Structuring Technique for Active Organic Devices, Karl Franzens Universität, Graz, Phd

[58] Andersson, P., Forchheimer, R., Tehrani, P., & Berggren, M. (2007). *Advanced Functional Materials*, *17*(16), 3074-3082.

[59] Deegan, R.D., Bakajin, O., Dupont, T.F., Huber, G., Nagel, S.R., Witten, T.A. (1997). *Nature 389* (6653): 827–829.

[60] Kim, Y. H., Sachse, C., Machala, M. L., May, C., Müller-Meskamp, L., & Leo, K. (2011). *Advanced Functional Materials*, *21*(6), 1076-1081.

[61] Zhang, X.-H., Potscavage, W. J., Choi, S., & Kippelen, B. (2009). *Applied Physics Letters*, *94*(4), 043312.

List of Figures